

Technical report 14-021

Synchronization of a Class of Cyclic Discrete-Event Systems Describing Legged Locomotion*

G. A. D. Lopes, B. Kersbergen, B. De Schutter, T. van den Boom, and
R. Babuška

To cite this work, please refer to the published version:

G. A. D. Lopes, B. Kersbergen, B. De Schutter, T. van den Boom, and R. Babuška,
“Synchronization of a class of cyclic discrete-event systems describing legged loco-
motion,” *Discrete Event Dynamic Systems: Theory and Applications*, vol. 26, no. 2,
pp. 225–261, 2016. doi:[10.1007/s10626-014-0206-6](https://doi.org/10.1007/s10626-014-0206-6)

Delft Center for Systems and Control
Delft University of Technology
Mekelweg 2, 2628 CD Delft
The Netherlands
phone: +31-15-278.24.73 (secretary)
URL: <https://www.dcsc.tudelft.nl>

* This report can also be downloaded via <https://dpub.eu/14-021>

Synchronization of a class of cyclic discrete-event systems describing legged locomotion

Gabriel A. D. Lopes, Bart Kersbergen, Bart De Schutter, Ton van den Boom, Robert Babuška

Delft University of Technology, Delft, The Netherlands

email: {g.a.delgadolopes,b.kersbergen,b.deschutter,a.j.j.vandenboom,r.babuska}@tudelft.nl

Abstract

It has been shown that max-plus linear systems are well suited for applications in synchronization and scheduling, such as the generation of train timetables, manufacturing, or traffic. In this paper we show that the same is true for multi-legged locomotion. In this framework, the max-plus eigenvalue of the system matrix represents the total cycle time, whereas the max-plus eigenvector dictates the steady-state behavior. Uniqueness of the eigenstructure also indicates uniqueness of the resulting behavior. For the particular case of legged locomotion, the movement of each leg is abstracted to two-state circuits: swing and stance (leg in flight and on the ground, respectively). The generation of a gait (a manner of walking) for a multi-legged robot is then achieved by synchronizing the multiple discrete-event cycles via the max-plus framework. By construction, different gaits and gait parameters can be safely interleaved by using different system matrices. In this paper we address both the transient and steady-state behavior for a class of gaits by presenting closed-form expressions for the max-plus eigenvalue and max-plus eigenvector of the system matrix and the coupling time. The significance of this result is in showing guaranteed stable gaits and gait switching, and also a systematic methodology for synthesizing controllers that allow for legged robots to change rhythms fast.

Keywords: Discrete-event systems, Max-plus algebra, Coupling time, Legged locomotion, Gait generation, Robotics

1 Introduction

Synchronization of cyclic processes is important in many fields, including manufacturing (Zhou et al. 1992), transportation (Heidergott and de Vries 2001), genomics (Shedden 2002), and neuroscience (Yamaguchi 2003; Holmes et al. 2006), etc (see references within (Dorfler and Bullo 2012)). In this paper we focus on a class of multiple concurrent two-state cyclic systems with a direct application to legged locomotion. Our motivation is the requirement of legged mobile robots to be able to switch between different gaits, without losing stability, when the environmental circumstances change or the requirements on the robot change, for example if a higher velocity is required.

Legged systems are traditionally modeled using cross-products of circles in the phase space of the set of continuous time gaits. Holmes et al. (2006) give an extensive review of dynamic legged locomotion. The Central pattern generator (Ijspeert 2008) approach to design motion controllers lies in assembling sets of error functions to be minimized that cross-relate the phases of multiple legs, resulting in attractive limit cycles for the desired gait.

Switching gaits online is typically not addressed since in the central pattern generator framework switching must be modeled as a hybrid system. Additionally, implementing “hard constraints” on the configuration space (Haynes et al. 2009) can be quite complex mainly due to the combinatorial nature of the gait space, and often it comes at the cost of dramatically increasing the complexity of the controller.

As an alternative to the common continuous time modeling approach, we introduce an abstraction to represent the combinatorial nature of the gait space for multi-legged robots into ordered sets of leg index numbers. This abstraction combined with max-plus linear equations allows for systematic synthesis and implementation of motion controllers for multi-legged robots where gait switching is natural and the translation to continuous-time motion controllers is straightforward (Lopes et al. 2014). The methodology presented is particularly relevant for robots with four, six, or higher numbers of legs where the combinatorial nature of the gait space plays an important role. For a large number of legs it is not obvious in which order each leg should be in swing or in stance. Most legged animals, in particular large mammals, are known to walk and

run with various gaits on a daily basis, depending on the terrain or how fast they need to move. The discrete-event framework presented in this paper enables the same behavior for multi-legged robots. Mathematical properties are derived for this framework, giving extra insight into the resulting robot motion.

The main mathematical representation employed in this paper are switching max-plus linear equations. By defining the state variables to represent the time at which events occur, systems of linear equations in the *max-plus algebra* (Cuninghame-Green 1979; Baccelli et al. 1992; Heidergott et al. 2006) can model a class of timed discrete-event systems. Specifically, max-plus linear systems are equivalent to (timed) Petri nets (Peterson 1981) where all places have a single incoming and a single outgoing arc. Max-plus linear systems inherit a large set of analysis and control synthesis tools thanks to many parallels between the max-plus-linear systems theory and the traditional linear systems theory. Discrete-event systems that enforce synchronization can be modeled in this framework. Max-plus algebra has been successfully applied to railroads (Braker 1991; Heidergott and de Vries 2001), queuing systems (Heidergott 2000), resource allocation (Gaubert and Mairesse 1998), and recently to image processing (Bede and Nobuhara 2009) and legged locomotion (Lopes G et al. 2009; Lopes et al. 2014).

The contributions of this paper are the following: we present a class of max-plus linear systems that realize schedules for the touchdown and lift-off of the legs for a given class of gaits. Next, we derive closed-form expressions for the max-plus eigenvalue and eigenvector of the system matrix, and show that the max-plus eigen-parameters are unique, implying a unique steady-state behavior. This result is then used to compute the coupling time, which characterizes the transient behavior. The importance of having closed-form expressions and uniqueness of the max-plus eigenstructure is that, not only can one compute these parameters very fast without resorting to simulations or numerical algorithms (e.g. Karp’s algorithm Baccelli et al. (1992)), but one also has guarantees of uniqueness: the motion of the robot will always converge in a finite number of steps to the behavior described by the current gait and its parameters, even after gait switches or temporary disturbances. In this paper we consider disturbances to be delayed lift-off and touchdown times, due to temporary obstructions. The class of max-plus-linear systems also ensure *kinematic stance stability*, that we define to be a required minimum of legs in stance that ensure the robot does not fall over during disturbances and gait switches. This reassurance is fundamental when designing gait controllers for robotics. Additionally we present a low maximum number of steps needed to reach steady-state motion after changing gaits. This paper is focused on the general mathematical properties of a class of discrete-event systems that describe legged locomotion, and not on the actual implementation of gait controllers for robots, as presented in Lopes et al. (2014).

In Section 2 we revisit the fundamentals of legged locomotion with special emphasis on gait generation and show that max-plus algebra can be used in the modeling of the synchronization of multiple legs. In Section 3 we briefly review relevant concepts from the theory of max-plus algebra and in Section 4 we present a class of parameterizations for the gait space. Given such a class, we derive a number of properties, such as the existence (Section 4.2) and uniqueness (Section 4.3) of the max-plus eigenstructure of the system matrices, and the coupling time (Section 4.4). We present simulations of switching gaits and disturbance rejection in Section 4.5 and conclude with Section 5. Figure 1 illustrates the structure of the contributions presented in this paper.

2 Modeling legged locomotion

In literature (Raibert 1986; Raibert M et al. 1989; Full and Koditschek D 1999; Holmes et al. 2006; Grillner S 2011), the study of legged locomotion is approached from two main directions: the signal generation side, where emphasis is placed on the classes of signals that result in periodic locomotion behavior independent of the physical platform; and the mechanics side, where the (hybrid) Newtonian mechanics models are analyzed independently of the driving control signal.

We focus on the first approach, by restating the traditional view of periodic gaits for legged systems being defined in the n -torus: Cartesian products of circles each representing an abstract phase that parameterizes the position of each leg in the Euclidean space. Such an abstraction serves as a platform for the models of “networks of phase oscillators” and central pattern generators, introduced in the earlier works of Grillner (1985) and Cohen et al. (1988). These are now accepted by both biology and robotics communities as standard modeling tools (Holmes et al. 2006).

In this paper we abstract beyond the notion of a continuous phase to consider the synchronization of discrete events. Taking a Petri net modeling approach, during ground locomotion the places represent leg stance (when the foot is touching the ground and supporting the body) and leg swing (when the foot and all parts of the leg are in the air). The transitions represent leg touchdown and lift off. This labeling is

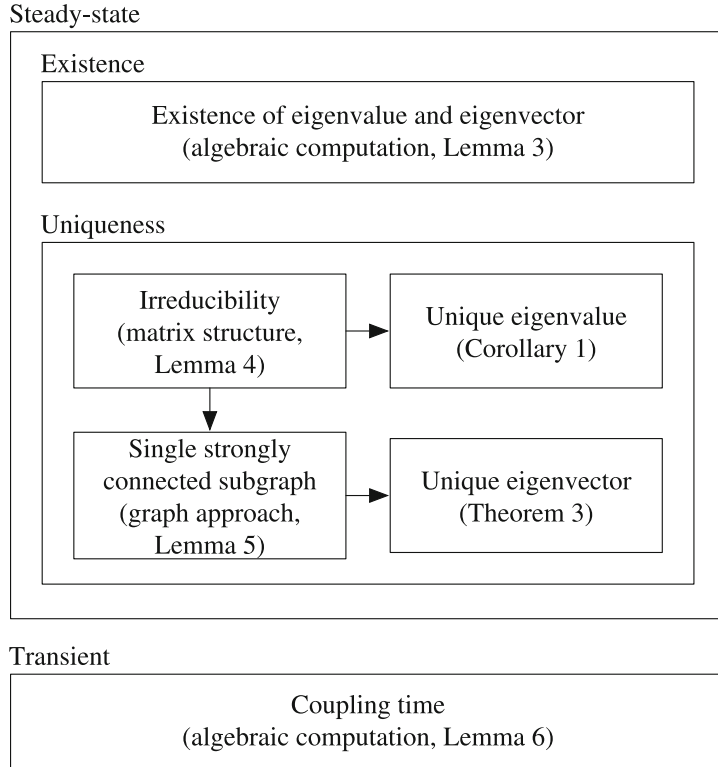


Figure 1: Structure of the contributions of this paper. We analyze both the steady-state and the transient behavior of a class of cyclic discrete-event systems that are well suited to model legged locomotion.

most convenient for ground locomotion, but one should be aware that the framework presented in this paper is valid for other types of locomotion where the phases of the various limbs need to be synchronized, such as swimming or flight. Figure 2 illustrates the conceptual difference between our approach (Fig. 2b) where each phase is represented by a single Petri net in the discrete-event systems domain and the traditional continuous phase central pattern generator (Fig. 2a). Here, phase synchronization is enforced on the torus by implementing controllers that achieve stable limit cycles (Klavins and Koditschek 2002). In this paper we translate timed event graphs¹ into the equivalent representation as max-plus linear systems, and achieve synchronization by designing the system matrices appropriately.

Consider the leg synchronization of a biped robot. In this case, only two legs need to be synchronized during locomotion. For a typical walking motion (no aerial phase) the left leg should only lift off the ground after the right leg has touched down, to make sure the robot does not fall due to lack of support. This synchronization requirement can be captured by introducing state variables for the transition events defined as follows: let $L_i(k)$ be the time instant leg i lifts off the ground and $t_i(k)$ be the time instant it touches the ground, both for k -th iteration, where k is considered to be a global event or “step” counter.

Enforcing that the time instant when the leg touches the ground must equal the time instant it lifted off the ground for the last time plus the time it is in swing (denoted τ_f) is realized by:

$$t_i(k) = L_i(k) + \tau_f. \quad (1)$$

A similar relation can be derived for the lift off time:

$$L_i(k) = t_i(k-1) + \tau_g, \quad (2)$$

where τ_g is the stance time and $t_i(k-1)$ refers to the previous iteration such that (1) and (2) can be used iteratively. For this system we have that $\tau_f > 0$ and also $\tau_g > 0$.

Synchronization of the cycles of two legs can be achieved by introducing a double stance time parameter, denoted τ_Δ , representing that after each leg touchdown both legs must stay in stance for at least τ_Δ time

¹We restrict ourselves to a class of timed Petri nets called *timed event graphs* such that a one-to-one translation to max-plus linear systems is possible (see Heidergott et al. (2006), chapter 7). In timed event graphs each place can have one single incoming arc and one single outgoing arc.

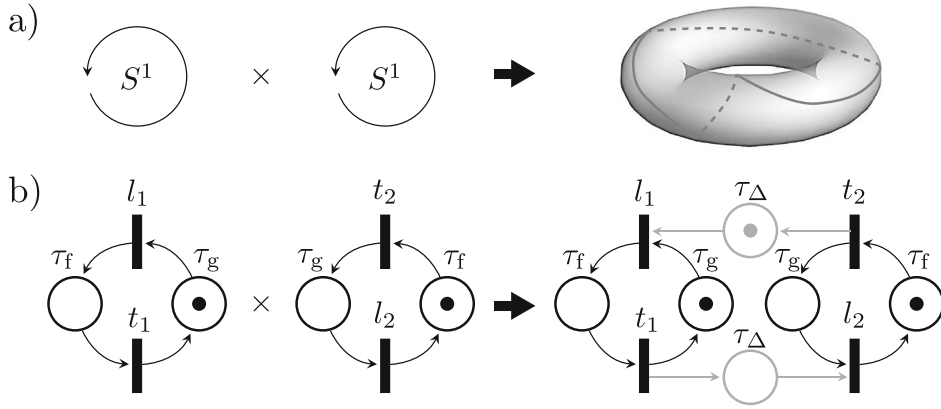


Figure 2: Modeling of legged locomotion. **(a)** The configuration space of two oscillators is a torus. Synchronization is achieved by constructing attractive limit cycles, represented by the curve on the torus. **(b)** Discrete-event representations of the phases of multiple oscillators can be modeled as multiple cyclic Petri nets. Synchronization is achieved by adding extra places, represented by the *gray circles* between t_2 and l_1 , and between t_1 and l_2 .

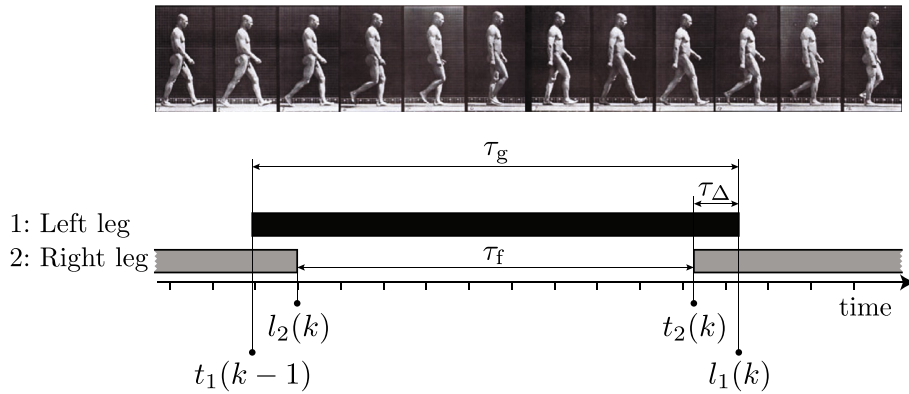


Figure 3: Illustration of a walking pattern, photos by Muybridge (1901). The *solid bars*, following Hildebrand’s diagram notation (Hildebrand, 1965), indicate that the leg is in stance (foot touching the ground) for τ_g time units, and white space that the leg is in swing (foot in flight) for τ_f time units. The time length when both feet are touching the ground is called the double-stance time τ_Δ . We use the notation $t_1(k-1)$ to represent the time instant when leg 1 (*left leg*) touches the ground, and $l_1(k)$ when it initiates a swing. The parameter k is the “step counter”.

units (see Fig. 3). This is captured by the following equations:

$$l_1(k) = \max(t_1(k-1) + \tau_g, t_2(k) + \tau_\Delta) \quad (3)$$

$$l_2(k) = \max(t_2(k-1) + \tau_g, t_1(k-1) + \tau_\Delta) \quad (4)$$

Equation 3 enforces simultaneously that leg 1 stays at least τ_g time units in stance and will only lift off at least τ_Δ time units after leg 2 has touched down. When both conditions are satisfied, lift off takes place. Equation 4 is analogous for leg 2.

Note that in this paper we analyze a class of nonlinear systems that realize schedules for the touchdown and lift-off of the legs for a given class of gaits, and here we do not consider its physical implementation. As such, the parameters τ_f , τ_g , and τ_Δ should be considered as design parameters indicating the desired stance, flight, and double stance time used to determine the schedule of touchdown and lift-off times.

Although the previous set of equations were designed for a walking behavior with no aerial phases, in practice they can also be used for running by choosing the double stance time to be negative, i.e. by enforcing that one leg lifts off τ_Δ time units before the other leg touches the ground. However, the results presented in this paper focus on the case when $\tau_\Delta \geq 0$ such that kinematic stance stability (in the sense of ensuring a desired minimum number of legs on the ground simultaneously) is guaranteed.

Equations 3 and 4 are non-linear, but rely only on the “max” and “plus” operations. This motivates the use of the theory of the max-plus algebra to find parsimonious discrete-event models for legged locomotion. The next section gives an introduction to the theory of max-plus linear algebra.

3 Max-plus algebra

In the early sixties of the 20th century the fact that certain classes of discrete-event systems can be described by models using the operations max and + was discovered independently by a number of researchers, among whom were Cuninghame-Green (1961, 1962) and Giffler (1960, 1963, 1968). These discrete-event systems are called max-plus-linear systems since the model that describes their behavior becomes “linear” when formulated in the max-plus algebra (Baccelli et al. 1992; Cuninghame-Green 1979; Heidergott et al. 2006), which has maximization and addition as its basic operations. More specifically, discrete-event systems in which only synchronization and no concurrency or choice occur (In a system in which choice or concurrency occurs, the order of two or more events depends on a choice made by an outside source, some events may only happen if certain choices are made) can be modeled using the operations maximization (corresponding to synchronization: a new operation starts as soon as all preceding operations have been finished) and addition (corresponding to the duration of activities: the finishing time of an operation equals the starting time plus the duration). Some examples of max-plus linear discrete-event systems are production systems, railroad networks, urban traffic networks, queuing systems, and array processors (Baccelli et al. 1992; Cuninghame-Green 1979; Heidergott et al. 2006).

An account of the pioneering work of Cuninghame-Green on max-plus system theory has been given in (Cuninghame-Green, 1979). Related work has been done by Gondran and Minoux (1976, 1984, 1987). In the eighties of the 20th century the topic attracted new interest due to the research of Cohen, Dubois, Moller, Quadrat, Viot (1983, 1985, 1989), Olsder (1986, 1988, 1990), and Gaubert (1990, 1992, 1993), which resulted in the publication of Baccelli et al. (1992). Since then, several other researchers have entered the field. For an historical overview we refer the interested reader to Gaubert and Plus (1997), Heidergott et al. (2006), De Schutter and van den Boom (2008).

In this section we give an introduction to the max-plus algebra and some notions of graph theory. This section is based on Baccelli et al. (1992), Cuninghame-Green (1979), where a complete overview of the max-plus algebra can be found.

3.1 Base definitions

The basic operations of the max-plus algebra are maximization and addition, which will be represented by \oplus and \otimes respectively

$$x \oplus y := \max(x, y) \quad \text{and} \quad x \otimes y := x + y$$

for $x, y \in \mathbb{R}_{\max} := \mathbb{R} \cup \{-\infty\}$. The zero element for \oplus in \mathbb{R}_{\max} is $\varepsilon := -\infty$ and the unit element for \otimes is $e := 0$.

The structure $(\mathbb{R}_{\max}, \oplus, \otimes)$ is called the max-plus algebra (Baccelli et al. 1992; Cuninghame-Green 1979). The operations \oplus and \otimes are called the max-plus-algebraic addition and max-plus-algebraic multiplication

respectively since many properties and concepts from linear algebra can be translated to the max-plus algebra by replacing $+$ by \oplus and \times by \otimes .

Throughout this paper the i, j element of a matrix A is denoted by $[A]_{ij}$. The matrix $\mathcal{E}_{m \times n}$ is the m by n max-plus zero matrix: $[\mathcal{E}_{m \times n}]_{ij} = \varepsilon$ for all i, j . The matrix E_n is the n by n max-plus identity matrix: $[E_n]_{ii} = e$ for all i and $[E_n]_{ij} = \varepsilon$ for all i, j with $i \neq j$. We also define the m by n max-plus “one” matrix $\mathbb{1}_{m \times n}$ such that $[\mathbb{1}]_{ij} = e = 0$ for all i, j . If the dimensions of $\mathcal{E}, E, \mathbb{1}$ are omitted in this paper, they should be clear from the context.

The basic max-plus-algebraic operations are extended to matrices as follows. If $A, B \in \mathbb{R}_{\max}^{m \times n}$, $C \in \mathbb{R}_{\max}^{n \times p}$ then

$$[A \oplus B]_{ij} = [A]_{ij} \oplus [B]_{ij} = \max([A]_{ij}, [B]_{ij}) \quad (5)$$

$$[A \otimes C]_{ij} = \bigoplus_{p=1}^n [A]_{ip} \otimes [C]_{pj} = \max_{p=1, \dots, n} ([A]_{ip} + [C]_{pj}), \quad (6)$$

for all i, j , where $\bigoplus_{p=1}^n a_p := \max_{p=1, \dots, n} (a_p)$. Note the analogy with the definitions of matrix sum and product in conventional linear algebra. The max-plus product of the scalar $\alpha \in \mathbb{R}_{\max}$ and the matrix $A \in \mathbb{R}_{\max}^{m \times n}$ is defined by $[\alpha \otimes A]_{ij} = \alpha \otimes [A]_{ij}$ for all i, j . The max-plus matrix power of $A \in \mathbb{R}_{\max}^{n \times n}$ is defined as follows: $A^{\otimes 0} = E_n$ and $A^{\otimes p} = A \otimes A^{\otimes p-1}$ for $p \geq 1$.

For $A, B \in \mathbb{R}_{\max}^{n \times m}$ we say that A *overcomes* B , written as $A \geq B$ if $A \oplus B = A$ (i.e., $[A]_{ij} \geq [B]_{ij}$ for all i, j).

3.2 Graphs

Before the rest of the properties and definitions of max-plus algebra can be described, some definitions from graph theory are needed. The graph theoretic concepts presented here are necessary for proving results regarding the uniqueness of eigenvectors. Such uniqueness implies a unique and predictable behavior of the robot gaits. First the definition of a directed graph is given:

Definition 1 (Directed graph). *A directed graph \mathcal{G} is defined as an ordered pair $(\mathcal{V}, \mathcal{A})$, where \mathcal{V} is a set of vertices and \mathcal{A} is a set of ordered pairs of vertices. The elements of \mathcal{A} are called arcs. A loop is an arc of the form (v, v) .*

A directed graph may contain several paths. A path is defined as:

Definition 2 (Path in a directed graph). *Let $\mathcal{G} = (\mathcal{V}, \mathcal{A})$ be a directed graph with $\mathcal{V} = \{v_1, v_2, \dots, v_n\}$. A path p of length l is a sequence of vertices $v_{i_1}, v_{i_2}, \dots, v_{i_{l+1}}$ such that $(v_{i_k}, v_{i_{k+1}}) \in \mathcal{A}$ for $k = 1, 2, \dots, l$. We represent this path by $v_{i_1} \rightarrow v_{i_2} \rightarrow \dots \rightarrow v_{i_{l+1}}$ and we denote the length of the path by $|p|_1 = l$. Vertex v_{i_1} is the initial vertex of the path and $v_{i_{l+1}}$ is the final vertex of the path.*

The set of all paths of length l from vertex v_{i_1} to v_{i_l} is denoted by $P(v_{i_1}, v_{i_l}; l)$. If for any two different vertices $v_i, v_j \in \mathcal{V}$ there exists a path from v_i to v_j then a directed graph $\mathcal{G} = (\mathcal{V}, \mathcal{A})$ is called *strongly connected*.

Some paths may have the same initial and final vertex, such paths are called circuits:

Definition 3 (Circuit in a directed graph). *Given a path $v_{i_1} \rightarrow v_{i_2} \rightarrow \dots \rightarrow v_{i_{l+1}}$, if $v_{i_1} = v_{i_{l+1}}$ this path is called a circuit.*

If no vertex in the circuit appears more than once, except for the initial vertex v_{i_1} , then this circuit is called an *elementary circuit*.

If we have a directed graph $\mathcal{G} = (\mathcal{V}, \mathcal{A})$ with $\mathcal{V} = \{1, 2, \dots, n\}$ and if we associate a real number $[A]_{ij}$ with each arc $(j, i) \in \mathcal{A}$, then we say that \mathcal{G} is a weighted directed graph. We call $[A]_{ij}$ the weight of the arc (j, i) . Note that the first subscript of $[A]_{ij}$ corresponds to the final (and not the initial) vertex of the arc (j, i) . This leads us to our next definition:

Definition 4 (Precedence graph). *Consider $A \in \mathbb{R}_{\max}^{n \times n}$. The precedence graph of A , denoted by $\mathcal{G}(A)$, is a weighted directed graph with vertices $1, 2, \dots, n$ and an arc (j, i) with weight $[A]_{ij}$ for each $[A]_{ij} \neq \varepsilon$.*

Let $A \in \mathbb{R}_{\max}^{n \times n}$ and consider $\mathcal{G}(A)$. The weight $|p|_w$ of a path $p : i_1 \rightarrow i_2 \rightarrow \dots \rightarrow i_{l+1}$ is defined as the sum of the weights of the arcs that compose the path: $|p|_w = [A]_{i_2 i_1} + [A]_{i_3 i_2} + \dots + [A]_{i_{l+1} i_l} = \bigotimes_{k=1}^l [A]_{i_{k+1} i_k}$. The average weight of a circuit is defined as the weight of the circuit divided by the length of the circuit:

$|p|_w/|p|_1$. Furthermore the element $[A^{\otimes p}]_{ij}$ is the maximum of the weights of all paths in the graph $\mathcal{G}(A)$ of length p from node j to node i :

$$[A^{\otimes p}]_{ij} = \bigoplus_{\{\rho:|\rho|_1=p;i_0=j;i_p=i\}} A_{i_p i_{p-1}} \otimes A_{i_{p-1} i_{p-2}} \otimes \cdots \otimes A_{i_1 i_0} \quad (7)$$

3.3 Properties of max-plus linear systems

Using the graph theoretical definitions presented in the previous section several properties of max-plus linear systems can be described. The important elements are the max-plus eigenvalues and eigenvectors, and the cyclicity of a matrix. These dictate the steady-state and transient behavior, respectively, of the evolution of max-plus linear systems that generate walking gaits.

Definition 5 (Irreducibility). *A matrix $A \in \mathbb{R}_{\max}^{n \times n}$ is called irreducible if its precedence graph is strongly connected.*

Using the definitions of the precedence graph and circuits the following theorem can be stated:

Theorem 1 (see Baccelli et al. (1992), Theorem 3.17). *Consider the following system of linear equations in the max-plus algebra:*

$$x = A \otimes x \oplus b \quad (8)$$

with $A \in \mathbb{R}_{\max}^{n \times n}$ and $b, x \in \mathbb{R}_{\max}^{n \times 1}$. *There exists a solution to this equation if there are only circuits of nonpositive weight (or no circuits at all) in $\mathcal{G}(A)$ and the solution is given by*

$$x = A^* \otimes b \quad (9)$$

where A^* is defined as

$$A^* := \bigoplus_{p=0}^{\infty} A^{\otimes p} \quad (10)$$

If the circuits have negative weight, or there are no circuits, this solution is unique.

In some cases the infinite max-plus sum in Eq. 10 can be limited to a finite number. This is the case if matrix A is nilpotent:

Definition 6 (Nilpotent matrix). *The matrix $A \in \mathbb{R}_{\max}^{n \times n}$ is called nilpotent if there exists a finite positive integer p_0 such that for all integers $p \geq p_0$ we have $A^{\otimes p} = \mathcal{E}$.*

One can verify that if $A \in \mathbb{R}_{\max}^{n \times n}$ is nilpotent then $p_0 \leq n$: If the precedence graph $\mathcal{G}(A)$ has a circuit of length l , $l \in \mathbb{N} \setminus \{0\}$ it also has a circuits of length $b \times l$, for $b \in \mathbb{N} \setminus \{0\}$, this means that $A^{b \times l}$ also has non- \mathcal{E} elements, since b goes up to infinity this proves that a matrix can only be nilpotent if its precedence graph $\mathcal{G}(A)$ has no circuits. If $\mathcal{G}(A)$ has no circuits, the length of its longest path can be at most $n - 1$, as a result no paths of length n or longer exist and therefore $A^{\otimes n} = \mathcal{E}$.

Using the graph theory we can give a clear interpretation of the max-plus eigenvalue and eigenvector. But first we need to define them:

Definition 7 (Max-plus eigenvalue and eigenvector). *Let $A \in \mathbb{R}_{\max}^{n \times n}$. If there exist a number $\lambda \in \mathbb{R}_{\max}$ and a vector $\nu \in \mathbb{R}_{\max}^n$ with $\nu \neq \varepsilon_{n \times 1}$ such that $A \otimes \nu = \lambda \otimes \nu$, then we say that λ is a max-plus eigenvalue of A and that ν is a corresponding max-plus eigenvector of A .*

It can be shown that every square matrix with entries in \mathbb{R}_{\max} has at least one max-plus eigenvalue (see e.g. Baccelli et al. (1992)). However, in contrast to linear algebra, the number of max-plus eigenvalues of an n by n matrix is in general less than n . If a matrix is irreducible, it has only one max-plus eigenvalue (see e.g. Cohen et al. (1985)). Moreover, if ν is a max-plus eigenvector of A , then $\alpha \otimes \nu$ with $\alpha \in \mathbb{R}$ is also a max-plus eigenvector of A .

The max-plus eigenvalue has the following graph-theoretic interpretation. Consider $A \in \mathbb{R}_{\max}^{n \times n}$. If λ_{\max} is the maximal average weight over all elementary circuits of $\mathcal{G}(A)$, then λ_{\max} is a max-plus eigenvalue of A . For formulas and algorithms to determine max-plus eigenvalues and eigenvectors the interested reader is referred to Baccelli et al. (1992), Braker and Olsder (1993), Cohen et al. (1985), Karp (1978) and the references cited therein. Every circuit of $\mathcal{G}(A)$ with an average weight that is equal to λ_{\max} is called a critical circuit.

Definition 8 (Critical graph and critical circuits). *The critical graph $\mathcal{G}^c(A)$ of the matrix A is the graph composed of all critical circuits.*

Another max-plus algebraic property related to the eigenvector and eigenvalue is the cyclicity of a matrix. The cyclicity is defined as:

Definition 9 (Cyclicity of a matrix). *A matrix A is said to be cyclic if there exists an eigenvalue $\lambda \in \mathbb{R}$, integers $c \in \mathbb{N}$ and $k_0 \in \mathbb{N}$ such that*

$$\forall p \geq k_0 : A^{\otimes p+c} = \lambda^{\otimes c} \otimes A^{\otimes p}. \quad (11)$$

The smallest c that satisfies this definition is called the cyclicity of matrix A , and k_0 is called the coupling time of A .

Theorem 2. *Any irreducible matrix A is cyclic, with cyclicity $c \in \mathbb{N}$, and coupling time k_0 .*

Proof. See e.g. Baccelli et al. (1992), Cohen et al. (1985), Gaubert (1994). □

For a system $x(k) = A \otimes x(k-1)$, with irreducible matrix A with cyclicity c and coupling time k_0 , the evolution of the vector $x(k)$ can be described as:

$$\begin{aligned} x(1) &= A \otimes x(0) \\ x(2) &= A \otimes x(1) = A \otimes A \otimes x(0) = A^{\otimes 2} \otimes x(0) \\ &\vdots \\ x(k_0) &= A^{\otimes k_0} \otimes x(0) \\ x(k_0 + 1) &= A^{k_0+1} \otimes x(0) \\ &\vdots \\ x(k_0 + c - 1) &= A^{k_0+c-1} \otimes x(0) \\ x(k_0 + c) &= A^{k_0+c} \otimes x(0). \end{aligned}$$

Using Eq. 11 $x(k_0 + c)$ can be rewritten as

$$x(k_0 + c) = \lambda^{\otimes c} \otimes A^{\otimes k_0} \otimes x(0) = \lambda^{\otimes c} \otimes x(k_0)$$

Clearly $x(k_0 + c)$ is just $x(k_0)$ (max-plus) multiplied by a constant $\lambda^{\otimes c}$. It can be concluded that starting from iteration k_0 the evolution of $x(k)$ is determined by the vectors $x(k_0), \dots, x(k_0 + c - 1)$. These vectors are repeated every c cycles with the only difference that they are (max-plus) multiplied by a constant $\lambda^{\otimes c}$ every c cycles. When the evolution of $x(k)$ can be described like this it is said that the system has reached a periodic regime. The coupling time k_0 of the system matrix is the number of iterations needed for the system to reach a periodic regime from any starting vector $x(0)$ and the cyclicity of the system matrix determines the number of vectors in the periodic regime.

This section has introduced the concepts of max-plus linear eigenvectors, that represent the cycle time of a gait; the max-plus eigenvalues, that represent the steady-state behavior of a gait; and the cyclicity of a system matrix that represents the transient behavior of a gait.

4 Legged locomotion via max-plus modeling

In this section we present a systematic procedure to generate time schedules for leg lift off and touchdown for a robot with $n \geq 2$ number of legs. In effect, we make use of the max-plus algebra tools presented in Section 3 to generalize the synchronization of two cyclic Petri nets Eqs. 1, 3 and 4, presented in Section 2. In order to achieve this generalization we start by proposing a specific *gait parameterization* in Section 4.1 from which a number of properties are later derived. We show how to construct the max-plus system equations in an implicit form using the gait parameterization. Next we verify that the resulting equations are solvable by demonstrating that the initially implicit max-plus system representation can be converted to an explicit one of the form $x(k) = A \otimes x(k-1)$. Given this equation it is fundamental to understand whether it reaches a unique steady state behavior. In robotics this is the equivalent of asking “does the robot walk/run as specified? If one of the legs gets blocked by an obstacle for a short time and therefore cannot move can

the robot recover from this?”. These questions are answered in Sections 4.2 (existence) and Section 4.3 (uniqueness) by analyzing the max-plus eigenstructure of the system matrix: a unique max-plus eigenvalue means that the legs have a unique cycle time, and a unique (up to scaling) max-plus eigenvector means that the legs always reach the same motion pattern, independently of the initial condition or temporary disturbances. In Section 4.4 we address the transient behavior of the max-plus linear system by looking at the coupling time of the system matrix. In practice this gives a number of transition steps required for a robot to switch gaits and reach steady-state. Finally in Section 4.5 we analyze gait switching and disturbance rejection for a quadruped robot, as an example of the applicability of the methodology presented here.

4.1 A gait parameterization

Consider the Eqs. 1, 3 and 4 described in Section 2 that describe the discrete-event dynamics of a synchronized 2 circuit Petri net. These can be rewritten in max-plus-linear algebra as:

$$t_i(k) = l_i(k) \otimes \tau_{\text{f}} \quad (12)$$

$$l_1(k) = t_1(k-1) \otimes \tau_{\text{g}} \oplus t_2(k) \otimes \tau_{\Delta} \quad (13)$$

$$l_2(k) = t_2(k-1) \otimes \tau_{\text{g}} \oplus t_1(k-1) \otimes \tau_{\Delta}. \quad (14)$$

These equations can be extended to robots with any number of legs and for many different gaits. Consider a general legged robot where a two-event circuit is associated to each leg. We present a parsimonious representation of a walking gait of a robot by grouping sets of legs and specifying in what order they are allowed to cycle.

Definition 10 (Leg partition). *Let n be the number of legs of the robot and define m as a number of leg groups. Let ℓ_1, \dots, ℓ_m be ordered sets of integers such that*

$$\bigcup_{p=1}^m \ell_p = \{1, \dots, n\}, \forall i \neq j, \ell_i \cap \ell_j = \emptyset, \text{ and } \forall i, \ell_i \neq \emptyset, \quad (15)$$

i.e., the sets ℓ_p form a partition of $\{1, \dots, n\}$.

Definition 11 (Gait and gait space). *A gait G is defined as an ordering relation of groups of legs:*

$$G = \ell_1 \prec \ell_2 \prec \dots \prec \ell_m. \quad (16)$$

The gait space is the set of all gaits that satisfy the previous definitions.

By considering that each ℓ_p contains the indices of a set of legs that are synchronized in phase, the previous ordering relation is interpreted in the following manner: the set of legs indexed by ℓ_i swings synchronously. Once all legs in ℓ_i touchdown and have been on the ground for at least τ_{Δ} time units then all legs in ℓ_{i+1} initiate their swing motion. The same is true for ℓ_m and ℓ_1 , closing the cycle. For example, a trotting gait, where diagonal pairs of legs move synchronously, for a quadruped robot as illustrated in Fig. 4, is represented by:

$$G_{\text{trot}} = \{1, 4\} \prec \{2, 3\}. \quad (17)$$

The gait space defined above can represent gaits for which all legs have the same cycle time. As such, gaits where one leg cycles twice while another cycles only once are not captured by this model. Examples of such gaits are not common, but have been used on hexapod robots to transverse very inclined slopes sideways (Weingarten et al. 2004).

For an n legged robot any gait in the gait space defined before can be described in max-plus algebra. First we can generalize Eqs. 12, 13 and 14 for n -legged robots by defining the following vectors:

$$t(k) = \begin{bmatrix} t_1(k) & \dots & t_n(k) \end{bmatrix}^T \quad (18)$$

$$l(k) = \begin{bmatrix} l_1(k) & \dots & l_n(k) \end{bmatrix}^T \quad (19)$$

Equation 12 is then written as:

$$t(k) = \tau_{\text{f}} \otimes l(k) \quad (20)$$

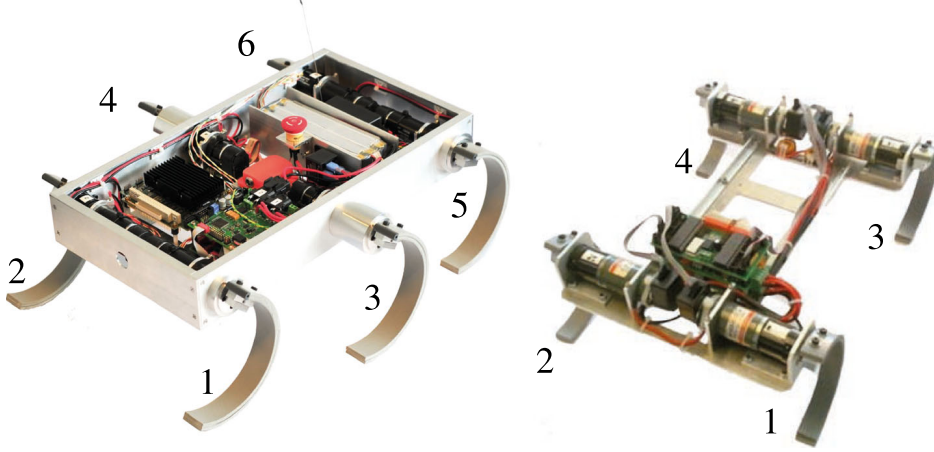


Figure 4: Walking robots with recirculating legs inspired by Saranli et al. (2001). Zebro robot on the *left* and RQuad on the *right* both developed at DCSC, Delft University of Technology. The numbers represent the leg index numbering assumed in this paper.

If one assumes that the synchronization is always enforced on the lift off time of a leg, Eqs. 13 and 14 are written jointly as:

$$l(k) = \tau_g \otimes t(k-1) \oplus P \otimes t(k) \oplus Q \otimes t(k-1) \quad (21)$$

where the matrices P and Q encode the synchronization between lift off of a leg related to a touchdown of the current event (as in Eq. 4) and a touchdown of the previous event (as in Eq. 3), respectively. With the previously defined gait notation matrices P and Q can be derived:

$$[P]_{pq} = \begin{cases} \tau_\Delta & \forall j \in \{1, \dots, m-1\}; \forall p \in \ell_{j+1}; \forall q \in \ell_j \\ \varepsilon & \text{otherwise.} \end{cases} \quad (22)$$

$$[Q]_{pq} = \begin{cases} \tau_\Delta & \forall p \in \ell_1; \forall q \in \ell_m \\ \varepsilon & \text{otherwise} \end{cases} \quad (23)$$

Matrix P ensures that the lift-off of the legs in ℓ_{j+1} in the current cycle is τ_Δ time units after the touchdown of the legs in ℓ_j in the current cycle (for all $j \in \{1, \dots, m-1\}$). Matrix Q ensures that the lift-off of the legs in ℓ_1 in the current cycle is after the touchdown of ℓ_m in the previous cycle. These matrices encode the synchronization between the sets of legs and ensure that only one set of legs can be in the air at all times, even during disturbances².

For the trotting gait G_{trot} we obtain:

$$P_{\text{trot}} = \begin{bmatrix} \varepsilon & \varepsilon & \varepsilon & \varepsilon \\ \tau_\Delta & \varepsilon & \varepsilon & \tau_\Delta \\ \tau_\Delta & \varepsilon & \varepsilon & \tau_\Delta \\ \varepsilon & \varepsilon & \varepsilon & \varepsilon \end{bmatrix} \quad \text{and} \quad Q_{\text{trot}} = \begin{bmatrix} \varepsilon & \tau_\Delta & \tau_\Delta & \varepsilon \\ \varepsilon & \varepsilon & \varepsilon & \varepsilon \\ \varepsilon & \varepsilon & \varepsilon & \varepsilon \\ \varepsilon & \tau_\Delta & \tau_\Delta & \varepsilon \end{bmatrix} \quad (24)$$

Using Eqs. 20–23 can be written in state-space form as:

$$\begin{bmatrix} t(k) \\ l(k) \end{bmatrix} = \begin{bmatrix} \mathcal{E} & \tau_i \otimes E \\ P & \mathcal{E} \end{bmatrix} \otimes \begin{bmatrix} t(k) \\ l(k) \end{bmatrix} \oplus \begin{bmatrix} E & \mathcal{E} \\ \tau_g \otimes E \oplus Q & E \end{bmatrix} \otimes \begin{bmatrix} t(k-1) \\ l(k-1) \end{bmatrix} \quad (25)$$

The rationale behind this particular model is to prevent that a legged platform has too many legs in swing while walking³ risking falling down. Synchronization constraints are always imposed on legs that are

²Disturbances are defined as time delays arising, for example, by a leg being stuck and not lifting off at the desired moment, or by a foot not touching down at the right time due to a hole on the ground.

³As mentioned previously in this paper we do not consider running, although it can still be achieved using the same class of models.

in stance and are about to enter swing: some legs should only swing if others are in stance (Eq. 21). By doing so we can ensure that, for any disturbance at most one group of legs is in swing and therefore we can guarantee that a minimum number of legs is always on the ground. This ensures kinematic stance stability, i.e. no matter which group of legs is in swing, the legs in the other groups ensure the robot has a stable pose due to its kinematics (e.g., the center of gravity lies inside the leg support polygon). Once in swing, legs are never constrained to go into stance (Eq. 20).

Define the matrices

$$A_0 = \left[\begin{array}{c|c} \mathcal{E} & \tau_f \otimes E \\ \hline P & \mathcal{E} \end{array} \right]; \quad A_1 = \left[\begin{array}{c|c} E & \mathcal{E} \\ \hline \tau_g \otimes E \oplus Q & E \end{array} \right], \quad (26)$$

and consider the full state x defined as

$$x(k) = [t^T(k) \ l^T(k)]^T.$$

Equation 25 can then be written in simplified notation:

$$x(k) = A_0 \otimes x(k) \oplus A_1 \otimes x(k-1). \quad (27)$$

Note that additional max-plus identity matrices E are introduced in the diagonal of matrix A_1 . This results in the extra trivial constraints $t_i(k) \geq t_i(k-1)$ and $l_i(k) \geq l_i(k-1)$, also resulting in the final system matrix (defined in Eq. 37 on page 12) being irreducible. This is observed later on in Lemma 4.

Define the function b that transforms a gait into a vector of integers:

$$b : \{[\ell_1]_1, \dots, [\ell_1]_{i_1}\} \prec \dots \prec \{[\ell_m]_1, \dots, [\ell_m]_{i_m}\} \mapsto \\ [[\ell_1]_1, \dots, [\ell_1]_{i_1} \dots [\ell_m]_1, \dots, [\ell_m]_{i_m}]^T. \quad (28)$$

Using again the previous trotting example we get that $b(G_{\text{trot}}) = [1 \ 4 \ 2 \ 3]^T$ (the symbol *flat* “ b ” is chosen since it “flattens” the ordered collection of ordered sets of a gait into a vector). Note that the gaits $\{1, 4\} \prec \{2, 3\}$ and $\{4, 1\} \prec \{2, 3\}$ although resulting in indistinguishable motion in practice, have different mathematical representations since $b(\{1, 4\} \prec \{2, 3\}) \neq b(\{4, 1\} \prec \{2, 3\})$.

Definition 12. A gait \bar{G} is called a normal gait if the elements of the vector $b(\bar{G})$ are sorted increasingly.

We show next that normal gaits result in well defined structures in the relevant max-plus matrices which facilitates the analysis. Since legs can be renamed without loss of generality, we introduce a leg relabeling procedure. For a gait G , define the similarity matrix $\bar{C} \in \mathbb{R}_{\max}^{n \times n}$ as:

$$[\bar{C}]_{ij} = \begin{cases} e & \text{if } [b(G)]_i = j \\ \varepsilon & \text{otherwise} \end{cases}, \forall i, j \in \{1, \dots, n\}. \quad (29)$$

The similarity matrix \bar{C} is such that

$$\bar{C} \otimes \bar{C}^T = \bar{C}^T \otimes \bar{C} = E.$$

The similarity matrix associated with the trotting gait G_{trot} is:

$$\bar{C}_{\text{trot}} = \begin{bmatrix} e & \varepsilon & \varepsilon & \varepsilon \\ \varepsilon & \varepsilon & \varepsilon & e \\ \varepsilon & e & \varepsilon & \varepsilon \\ \varepsilon & \varepsilon & e & \varepsilon \end{bmatrix} = \begin{bmatrix} 0 & -\infty & -\infty & -\infty \\ -\infty & -\infty & -\infty & 0 \\ -\infty & 0 & -\infty & -\infty \\ -\infty & -\infty & 0 & -\infty \end{bmatrix}, \quad (30)$$

here written in both max-plus and traditional algebra notation for legibility purposes. The similarity matrix \bar{C} has the property of “normalizing” the P and Q matrices to a max-plus algebraic lower block triangular form \bar{P} and a max-plus algebraic upper block triangular form \bar{Q} respectively:

$$\bar{P} = \bar{C} \otimes P \otimes \bar{C}^T \quad (31)$$

$$\bar{Q} = \bar{C} \otimes Q \otimes \bar{C}^T \quad (32)$$

Taking the previous example of the trotting gait, the normalized matrices take the form

$$\bar{P}_{\text{trot}} = \begin{bmatrix} \varepsilon & \varepsilon & \varepsilon & \varepsilon \\ \varepsilon & \varepsilon & \varepsilon & \varepsilon \\ \tau_{\Delta} & \tau_{\Delta} & \varepsilon & \varepsilon \\ \tau_{\Delta} & \tau_{\Delta} & \varepsilon & \varepsilon \end{bmatrix} \text{ and } \bar{Q}_{\text{trot}} = \begin{bmatrix} \varepsilon & \varepsilon & \tau_{\Delta} & \tau_{\Delta} \\ \varepsilon & \varepsilon & \tau_{\Delta} & \tau_{\Delta} \\ \varepsilon & \varepsilon & \varepsilon & \varepsilon \\ \varepsilon & \varepsilon & \varepsilon & \varepsilon \end{bmatrix}, \quad (33)$$

which are generated by the normal gait $\{1, 2\} \prec \{3, 4\}$. Let $\#\ell_i$ represent the number of elements of the set ℓ_i . For a general normal gait

$$\bar{G} = \ell_1 \prec \ell_2 \prec \dots \prec \ell_m \quad (34)$$

with $\bar{\mathbb{1}}_{i,j} = \mathbb{1}_{\#\ell_i \times \#\ell_j}$ the structure of the matrices \bar{P} and \bar{Q} is:

$$\bar{P} = \begin{bmatrix} \varepsilon & & \dots & \varepsilon \\ \tau_{\Delta} \otimes \bar{\mathbb{1}}_{2,1} & \varepsilon & & \vdots \\ \varepsilon & \tau_{\Delta} \otimes \bar{\mathbb{1}}_{3,2} & \varepsilon & \\ \vdots & & \ddots & \\ \varepsilon & \dots & \tau_{\Delta} \otimes \bar{\mathbb{1}}_{m,m-1} & \varepsilon \end{bmatrix} \quad (35)$$

$$\bar{Q} = \begin{bmatrix} \varepsilon & \tau_{\Delta} \otimes \bar{\mathbb{1}}_{1,m} \\ \varepsilon & \varepsilon \end{bmatrix}. \quad (36)$$

From Eq. 35 it is clear that the matrix \bar{P} is always max-plus nilpotent, since the upper triangle is max-plus zero.

Lemma 1. *Max-plus nilpotency is invariant to max-plus similarity transformations (e.g. as defined in Eqs. 31, 32).*

Proof. See Appendix A.1 on page 17. □

Given an arbitrary gait G with associated matrices P , Q , A_0 , and A_1 one can find the normal matrix \bar{P} which is max-plus nilpotent. From Lemma 1 then P is also max-plus nilpotent.

Lemma 2. *A sufficient condition for A_0^* to exist is that the matrix P is nilpotent in the max-plus sense.*

Proof. See Appendix A.2 on page 17. □

Since P is always max-plus nilpotent for gaits generated by expressions (22) and (23), we conclude that A_0^* is well defined. In the beginning of Section 4 we have presented the synchronization (27) implicitly. However, if A_0^* exists then using Eqs. 8 and 9, system (27) can be transformed into an explicit set of equations. Let A , which we call system matrix, be defined by:

$$A = A_0^* \otimes A_1. \quad (37)$$

Using Theorem 1 Eq. 27 can be rewritten as:

$$\begin{aligned} x(k) &= A_0^* \otimes A_1 \otimes x(k-1) \\ &= A \otimes x(k-1). \end{aligned} \quad (38)$$

With the system matrix A defined we can use the max-plus theory from Section 3 to analyze the behavior of the system described in Eq. 38.

4.2 Existence of max-plus eigenstructure

The results obtained below use various analysis techniques available for max-plus linear systems. This is necessary due to the intrinsic time structure associated with the problem. Petri net tools (e.g., incidence matrices) can be used to understand structural properties of the system, such as irreducibility, but temporal properties are better analyzed using max-plus linear tools. In Section 4.3 we show that for a fixed structure (i.e., a single Petri net) unique or non-unique eigenvectors are found by changing the holding time parameters. This result could not be captured by the Petri net structure alone. The analysis steps presented from here on are summarized in Fig. 1.

Consider the following assumption (which is always satisfied in practice since the leg swing and stance times are always positive numbers):

Assumption A1. $\tau_g, \tau_f > 0$.

Furthermore let:

$$\tau_\delta = \tau_f \otimes \tau_\Delta \text{ and } \tau_\gamma = \tau_f \otimes \tau_g \quad (39)$$

Then the following lemma defines an eigenvalue and eigenvector for the system matrix A .

Lemma 3. *If Assumption A1 is satisfied then*

$$\lambda := \tau_\delta^{\otimes m} \otimes \tau_\gamma \quad (40)$$

is a max-plus eigenvalue of the system matrix A (and \bar{A}) defined by Eq. 38 (and Eqs. 90–93), and $\nu \in \mathbb{R}_{\max}^{2n}$ defined by

$$\forall j \in \{1, \dots, m\}, \forall q \in lj : [\nu]_q := \tau_f \otimes \tau_\delta^{\otimes j-1} \quad (41)$$

$$[\nu]_{q+n} := \tau_\delta^{\otimes j-1} \quad (42)$$

is a max-plus eigenvector of A .

Proof. See Appendix A.3 on page 18. □

Consider again the trotting gait for a quadruped G_{trot} defined in Eq. 17. For this gait $m = 2$, resulting in:

$$\nu_{\text{trot}} = \begin{bmatrix} \tau_f \\ \tau_\Delta \otimes \tau_f^{\otimes 2} \\ \tau_\Delta \otimes \tau_f^{\otimes 2} \\ \tau_f \\ 0 \\ \tau_\Delta \otimes \tau_f \\ \tau_\Delta \otimes \tau_f \\ 0 \end{bmatrix}; \quad \lambda_{\text{trot}} = (\tau_f \otimes \tau_\Delta)^{\otimes 2} \oplus \tau_f \otimes \tau_g. \quad (43)$$

4.3 Uniqueness of max-plus eigenstructure

Lemma 4. *Matrix A is irreducible.*

Proof. See Appendix A.4 on page 19. □

Corollary 1. *The max-plus eigenvalue λ of A is given by Eq. 40 is unique.*

The max-plus eigenvector ν defined by Eqs. 41–42 is not necessarily unique, given assumption A1 alone. To the authors' best knowledge, there exists only a graphical test to prove the uniqueness of the max-plus eigenvector in general (no algebraic method exist). As such we take advantage of the critical graph of A to further investigate this property. If the critical graph of an irreducible max-plus system matrix has a single strongly connected subgraph, then its max-plus eigenvector is unique up to a max-plus scaling factor (see Baccelli et al. (1992), Theorem 3.101). We proceed by computing the critical graph(s) of \bar{A} .

Before we look at the critical graph of A we first use a similarity transformation on A to get \bar{A} and then we look at the critical graph of \bar{A} . The critical graphs of A and \bar{A} are equivalent up to a label renaming. Therefore properties derived from the critical graph of \bar{A} are also valid for A . For more details on the similarity transformation of A into \bar{A} the reader is referred to Appendix B.

The critical graph of \bar{A} is given in Fig. 5 for the three different possibilities of the eigenvalue: $\lambda = \tau_\gamma = \tau_\delta^{\otimes m}$, $\lambda = \tau_\delta^{\otimes m} > \tau_\gamma$, and $\lambda = \tau_\gamma > \tau_\delta^{\otimes m}$. The critical graph has been derived from the precedence graph of \bar{A} , this process has been described in Appendix C.

Consider the following assumption:

Assumption A2. $\tau_\gamma \leq \tau_\delta^{\otimes m}$.

Lemma 5. *If Assumption A2 is verified then the critical graph of $\mathcal{G}^c(A)$ (and $\mathcal{G}^c(\bar{A})$) has a single strongly connected subgraph.*

Proof. This can be seen in Fig. 5 and is formally proven in Appendix A.5, page 19. □

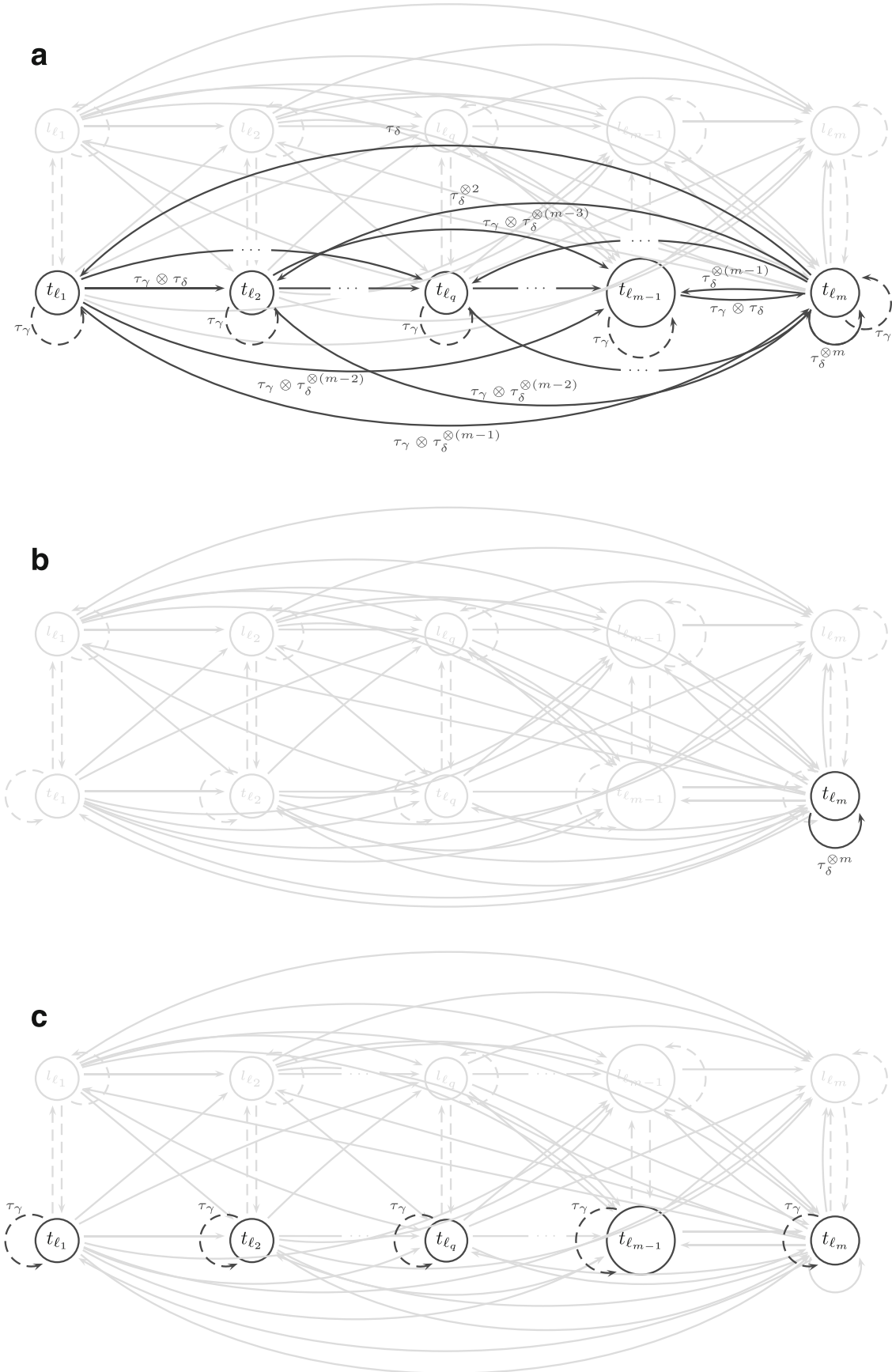


Figure 5: Critical graphs of the system matrix \bar{A} highlighted in black. **a)** Case 1: $\tau_\gamma = \tau_\delta^{\otimes m} = \lambda$. **b)** Case 2: $\tau_\gamma < \tau_\delta^{\otimes m} = \lambda$. **c)** Case 3: $\tau_\delta^{\otimes m} < \tau_\gamma = \lambda$.

In Fig. 5 the critical graph of \bar{A} is given by the black nodes and vertices, the gray nodes and vertices are the nodes and vertices of the precedence graph that do not belong to the critical graph. For the case that $\tau_\gamma = \tau_\delta^{\otimes m} = \lambda$ (Fig. 5a) and $\tau_\gamma < \tau_\delta^{\otimes m} = \lambda$ (Fig. 5b) there is a path from all nodes of the critical graph to the other nodes, this means the critical graph consists of a single strongly connected subgraph and therefore the eigenvector is unique. For the case that $\tau_\delta^{\otimes m} < \tau_\gamma = \lambda$ (Fig. 5c), there are only paths from the nodes to themselves and therefore the critical graph consists of several strongly connected subgraphs and the eigenvector is not unique.

The previous lemma leads to the following theorem about the uniqueness of the eigenvalue and eigenvector:

Theorem 3. *Given Assumptions A1 and A2, the max-plus eigenvalue λ of the system matrix A (and \bar{A}), defined by Eq. 40, is unique, and the max-plus eigenvector ν of A (and \bar{A}), defined by Eqs. 41-42 is unique up to a max-plus scaling factor.*

Proof. See Appendix A.6 on page 22. □

4.4 Coupling time

Theorem 2 on page 8 describes an important property of max-plus-linear systems when the system matrix A is irreducible: it guarantees the existence of an autonomous steady-state regime that is achieved in a number of finite steps k_0 , called the *coupling time*. Computing the coupling time is very important for the application of legged locomotion since it provides the number of steps a robot needs to take to reach steady state after a gait transition or a perturbation.

Lemma 6. *Given Assumptions A1, A2, the coupling time for the max-plus-linear system defined by Eq. 25 is $k_0 = 2$ with cyclicity $c = 1$.*

Proof. See Appendix A.7 on page 22. □

Next we show how these properties affect the transient behavior of the system when switching gaits.

4.5 Switching gaits and disturbance rejection

Due to the event-driven nature of the models used in this paper and the use of the max operator for enforcing synchronization between circuits, certain events are only allowed to fire if a set of other events has fired previously. This enforces by construction that, for example, if a leg is swinging and its foot does not touch the ground at the desired time, then all the other connected leg lift off events that succeed this touchdown event are not allowed to fire. In practice there cannot be a situation where the robot falls down from lack of support. This applies in general to every sequence of connected events via a holding time. As such, gait switching and disturbances by means of event firing delays are safe by construction. In this section we present two simulations of the proposed switching max-plus-linear system for a quadruped robot to illustrate this safety by construction properties in practice.

The first simulation address switching from a trot to a walking gait. The trotting gait has already been described in Eq. 17 and its eigenvector and eigenvalue in Eq. 43. The walking gait is represented by

$$G_{\text{walk}} = \{1\} \prec \{4\} \prec \{2\} \prec \{3\}.$$

With the gait given we can use Eqs. 40, 41, and 42 to determine the eigenvalue and eigenvector of the gait:

$$v_{\text{walk}} = \begin{bmatrix} \tau_{\text{f}} \\ (\tau_{\Delta} \otimes \tau_{\text{f}})^{\otimes 2} \otimes \tau_{\text{f}} \\ (\tau_{\Delta} \otimes \tau_{\text{f}})^{\otimes 3} \otimes \tau_{\text{f}} \\ \tau_{\Delta} \otimes \tau_{\text{f}}^{\otimes 2} \\ 0 \\ (\tau_{\Delta} \otimes \tau_{\text{f}})^{\otimes 2} \\ (\tau_{\Delta} \otimes \tau_{\text{f}})^{\otimes 3} \\ \tau_{\Delta} \otimes \tau_{\text{f}} \end{bmatrix}; \quad \lambda_{\text{walk}} = (\tau_{\text{f}} \otimes \tau_{\Delta})^{\otimes 4} \oplus \tau_{\text{f}} \otimes \tau_{\text{g}}. \quad (44)$$

For the simulation of the gait switch we use the parameters described in the following table:

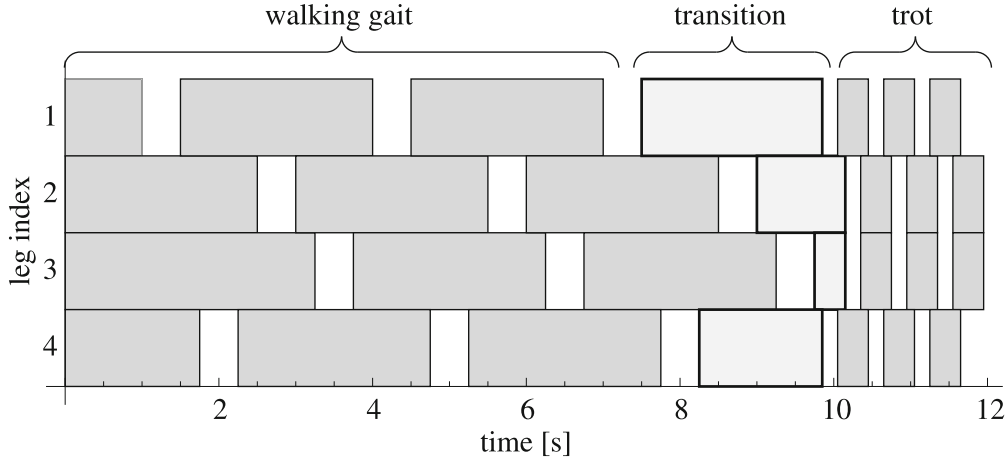


Figure 6: Simulation of gait patterns for a quadruped robot. A safe transition occurs between a walk and trot gaits.

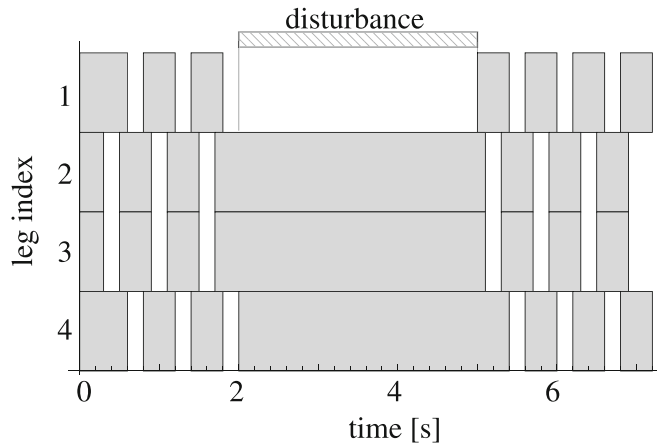


Figure 7: Simulation of a trotting gait pattern for a quadruped robot. At $t = 2$ s a disturbance is introduced in the first leg. The remaining legs stay in stance until the disturbance subsides and leg 1 returns to stance.

Parameter	Walk	Trot
τ_g	1	0.3
τ_f	0.5	0.2
τ_Δ	0.25	0.1

In the simulation the system is initialized by assuming all legs are on the ground, therefore the starting vector is set to

$$x(0) = \begin{bmatrix} 0 & 0 & 0 & 0 & \varepsilon & \varepsilon & \varepsilon & \varepsilon \end{bmatrix}^T.$$

The simulation, illustrated in Fig. 6, starts with the walking gait. After 3 cycles it switches to the trotting gait and continue for 3 more cycles.

It is clear from the simulation that the switching max-plus-linear system reaches the steady state behavior of the walking gait, as described above, at the end of the first cycle. After the gait switch at the end of cycle three the robot only needs one cycle (typically two) to reach the steady state behavior of the trotting gait, and during the transition the only legs that are in the air at the same time are legs of a single group of legs of the trotting gait.

In the next simulation we show the result of one of the legs when disturbed by being forced to stay longer in the air. Once more, the system uses the trotting gait as described in Eq. 17. The results of this simulation are shown in Fig. 7.

It is visible from the simulation that the lift-off of the undisturbed set of legs is postponed until the leg that is stuck in the air touches down plus an extra τ_δ time units. This shows that the proposed system can

ensure that a minimal number of legs remain on the ground even during disturbances.

5 Conclusions

This paper addresses the generation of leg lift off and touchdown time schedules for legged robots with many legs. We propose a different approach from the standard CPG methods by abstracting and using discrete-event circuits to model the phases of a leg while walking: swing and stance. The models are written as a set of max-plus linear systems where the state variables represent the leg lift off and touchdown times. The result of the evolution of the discrete-event dynamical system is a time schedule for the legs.

We proposed a gait parameterization that generates a gait space, where each gait represents an ordered sequence of swing actions for the legs. The combinatorial nature of this gait space (also present in any other gait spaces), arising from all the possible arrangements in which multiple legs can be synchronized, is captured by a compact representation as an ordered set of ordered sets. Using this gait parameterization important structural properties of the max-plus system matrix are obtained in closed-form. We demonstrate using algebraic and graph theoretic arguments that the max-plus eigenvectors and eigenvalues of the system matrix exist and are unique. The implication of this fact is a unique steady state behavior for the time schedule associated with each gait. In practice this means that a legged robot controlled by the max-plus generated time schedule follows a consistent and predictable gait pattern.

The coupling time is computed in closed form, revealing the transient response to gait switching or disturbances. Since the coupling time was found to be two, we have shown that legged robots can switch gaits (or rhythms), without having to stop the robot, in at most two leg cycles. Moreover, gait switching is kinematic stance stable, an important property to prevent robots falling down while switching gaits.

In the derivation process we have found that similarity transformations can facilitate the algebraic manipulations by exposing the structure of the system matrices. This was important to find closed-form expressions to the eigenstructure of the system and the coupling time, that typically need to be computed via simulations or using numerical procedures. On the graph side, the node-reduction procedure has allowed depicting graphs that can have an arbitrary large number of nodes. A graph-theoretic proof is needed for proving the uniqueness of the max-plus eigenvector. Our results are valid for robots with an arbitrary number of legs.

Further research will look towards relaxing the structure of the system matrix to address the synchronization of general cyclic systems and towards the modeling of more general gaits.

A Proofs

A.1 Proof of Lemma 1

Proof. Let \bar{P} be nilpotent and \bar{C} be a similarity matrix. Let $P = \bar{C}^T \otimes \bar{P} \otimes \bar{C}$. As such

$$\begin{aligned} P^{\otimes p} &= (\bar{C}^T \otimes \bar{P} \otimes \bar{C})^{\otimes p} = \\ &= \bar{C}^T \otimes \bar{P} \otimes \bar{C} \otimes \bar{C}^T \otimes \bar{P} \otimes \bar{C} \otimes \dots \otimes \bar{C}^T \otimes \bar{P} \otimes \bar{C} \\ &= \bar{C}^T \otimes \bar{P}^{\otimes p} \otimes \bar{C} \end{aligned}$$

and,

$$\exists p_0 > 0, \forall p \geq p_0 : P^{\otimes p} = \bar{C}^T \otimes \bar{P}^{\otimes p} \otimes \bar{C} = \mathcal{E}$$

□

A.2 Proof of Lemma 2

Proof. By direct computation, the repetitive products of A_0 can be found to be

$$A_0^{\otimes p} = \begin{cases} \left[\begin{array}{c|c} \mathcal{E} & \tau_f^{\otimes \frac{p+1}{2}} \otimes P^{\otimes \frac{p-1}{2}} \\ \hline \tau_f^{\otimes \frac{p-1}{2}} \oplus P^{\otimes \frac{p+1}{2}} & \mathcal{E} \end{array} \right] & \text{if } p \text{ is odd} \\ \left[\begin{array}{c|c} \tau_f^{\otimes \frac{p}{2}} \otimes P^{\otimes \frac{p}{2}} & \mathcal{E} \\ \hline \mathcal{E} & \tau_f^{\otimes \frac{p}{2}} \otimes P^{\otimes \frac{p}{2}} \end{array} \right] & \text{if } p \text{ is even} \end{cases} \quad (45)$$

If P is max-plus nilpotent, then there exists a finite positive integer p_0 such that $\forall p \geq p_0 : P^{\otimes p} = \mathcal{E} \Rightarrow A_0^{\otimes(2p+1)} = \mathcal{E}$, and therefore the max-plus sum for the computation of A_0 is finite:

$$A_0^* = \bigoplus_{q=0}^{\infty} A_0^{\otimes q} = \bigoplus_{q=0}^{2p} A_0^{\otimes q}. \quad (46)$$

□

A.3 Proof of Lemma 3

Proof. With $\nu \in \mathbb{R}_{\max}^n$, let $[\bar{\nu}]_q = [\nu]_{q+n}$ for all j and $q \in \ell_j$. Then $\nu = \left[(\tau_{\mathbb{f}} \otimes \bar{\nu})^T \quad \bar{\nu}^T \right]^T$. Recall Eqs. 8 and 9 with new variables z and B such that $z = B \otimes z \oplus b$ with solution $z = B^* \otimes b$. Now let $z = \lambda \otimes \nu$, $B = A_0$, and $b = A_1 \otimes \nu$. We obtain

$$\lambda \otimes \nu = A_0 \otimes \lambda \otimes \nu \oplus A_1 \otimes \nu = A_0 \otimes A_1 \otimes \nu = A \otimes \nu$$

Given the previous result, it is sufficient to show that if λ and ν are a max-plus eigenvalue and eigenvector of A respectively, then replacing the state variable $x(k-1)$ by ν and $x(k)$ by $\lambda \otimes \nu$ in Eq. 25 holds true:

$$\begin{aligned} \lambda \otimes \nu &= \lambda \otimes \begin{bmatrix} \tau_{\mathbb{f}} \otimes \bar{\nu} \\ \bar{\nu} \end{bmatrix} = \lambda \otimes \left[\begin{array}{c|c} \mathcal{E} & \tau_{\mathbb{f}} \otimes E \\ \hline P & \mathcal{E} \end{array} \right] \otimes \nu \oplus \left[\begin{array}{c|c} E & \mathcal{E} \\ \hline \tau_{\mathbb{g}} \otimes E \oplus Q & E \end{array} \right] \otimes \nu \\ &= \left[\begin{array}{c|c} E & \lambda \otimes \tau_{\mathbb{f}} \otimes E \\ \hline \lambda \otimes P \oplus \tau_{\mathbb{g}} \otimes E \oplus Q & E \end{array} \right] \otimes \begin{bmatrix} \tau_{\mathbb{f}} \otimes \bar{\nu} \\ \bar{\nu} \end{bmatrix}. \end{aligned}$$

The previous expression is equivalent to the following two equations:

$$\lambda \otimes \tau_{\mathbb{f}} \otimes \bar{\nu} = \tau_{\mathbb{f}} \otimes \bar{\nu} \oplus \lambda \otimes \tau_{\mathbb{f}} \otimes \bar{\nu} \quad (47)$$

$$\lambda \otimes \bar{\nu} = \tau_{\mathbb{f}} \otimes (\lambda \otimes P \oplus \tau_{\mathbb{g}} \otimes E \oplus Q) \otimes \bar{\nu} \oplus \bar{\nu}. \quad (48)$$

Since $\lambda > 0$ (by Assumption A1), (47) is always verified. Thus we focus on Eq. 48, which can be simplified due to $\tau_{\mathbb{f}} \otimes \tau_{\mathbb{g}} > 0$:

$$\lambda \otimes \bar{\nu} = (\tau_{\mathbb{f}} \otimes \tau_{\mathbb{g}}) \otimes \bar{\nu} \oplus \tau_{\mathbb{f}} \otimes (\lambda \otimes P \oplus Q) \otimes \bar{\nu}. \quad (49)$$

Let $\tau_{\Delta} \otimes P_0 = P$ and $\tau_{\Delta} \otimes Q_0 = Q$, i.e., all entries of matrices P_0 and Q_0 are either e or ε to obtain (recall that $\tau_{\delta} = \tau_{\mathbb{f}} \otimes \tau_{\Delta}$ and $\tau_{\gamma} = \tau_{\mathbb{f}} \otimes \tau_{\mathbb{g}}$):

$$\lambda \otimes \bar{\nu} = \tau_{\gamma} \otimes \bar{\nu} \oplus \tau_{\delta} \otimes (\lambda \otimes P_0 \oplus Q_0) \otimes \bar{\nu}. \quad (50)$$

We now consider two cases:

- i) First we analyze the row indices of Eq. 50 that are elements of the sets ℓ_2, \dots, ℓ_m . For each $j \in \{1, \dots, m-1\}$ and for each row $p \in \ell_{j+1}$ we obtain (notice that according to Eq. 23) all the elements of $[Q_0]_{p,\cdot}$ are ε since $p \notin \ell_1$, and that $[\bar{\nu}]_p = \tau_{\delta}^{\otimes j}$ for $p \in \ell_{j+1}$):

$$[\lambda \otimes \bar{\nu}]_p = [\tau_{\gamma} \otimes \bar{\nu}]_p \oplus \tau_{\delta} \otimes [\lambda \otimes P_0 \oplus Q_0 \otimes \bar{\nu}]_p \Leftrightarrow \quad (51)$$

$$\lambda \otimes [\bar{\nu}]_p = \tau_{\gamma} \otimes [\bar{\nu}]_p \oplus \tau_{\delta} \otimes [\lambda \otimes P_0]_{p,\cdot} \otimes \underbrace{\bar{\nu} \oplus [Q_0]_{p,\cdot}}_{\varepsilon} \otimes \bar{\nu} \Leftrightarrow \quad (52)$$

$$\lambda \otimes \tau_{\delta}^{\otimes j} = \tau_{\gamma} \otimes \tau_{\delta}^{\otimes j} \oplus \tau_{\delta} \otimes \bigoplus_{q \in \ell_j} \lambda \otimes \underbrace{[P_0]_{p,q}}_{\varepsilon} \otimes [\bar{\nu}]_q \Leftrightarrow \quad (53)$$

$$\lambda \otimes \tau_{\delta}^{\otimes j} = \tau_{\gamma} \otimes \tau_{\delta}^{\otimes j} \oplus \tau_{\delta} \otimes \lambda \otimes \tau_{\delta}^{\otimes j-1} \Leftrightarrow \quad (54)$$

$$\lambda \otimes \tau_{\delta}^{\otimes j} = \tau_{\gamma} \otimes \tau_{\delta}^{\otimes j} \oplus \lambda \otimes \tau_{\delta}^{\otimes j}. \quad (55)$$

The last term always holds true since $\lambda \geq \tau_{\gamma}$. Thus for rows $p \in \ell_2, \dots, \ell_m$ Eq. 50 holds true.

ii) We now look at all the remaining rows p such that $p \in \ell_1$ (noticing now that according to (22) all the elements of $[P_0]_{p..}$ are ε and that $[\bar{\nu}]_p = e$ since $p \in \ell_1$):

$$[\lambda \otimes \bar{\nu}]_p = [\tau_\gamma \otimes \bar{\nu}]_p \oplus \tau_\delta \otimes [\lambda \otimes P_0 \oplus Q_0]_{p..} \otimes \bar{\nu} \Leftrightarrow \quad (56)$$

$$\lambda \otimes [\bar{\nu}]_p = \tau_\gamma \oplus \tau_\delta \otimes \underbrace{[\lambda \otimes P_0]_{p..}}_\varepsilon \otimes \bar{\nu} \oplus \tau_\delta \otimes [Q_0]_{p..} \otimes \bar{\nu} \Leftrightarrow \quad (57)$$

$$\lambda = \tau_\gamma \oplus \tau - \delta \otimes \bigoplus_{q \in \ell_m} \underbrace{[Q_0]_{p,q}}_e \otimes [\bar{\nu}]_q \Leftrightarrow \quad (58)$$

$$\lambda = \tau_\gamma \oplus \tau_\delta \otimes \tau_\delta^{\otimes m-1} \Leftrightarrow \quad (59)$$

$$\lambda = \tau_\gamma \oplus \tau_\delta^{\otimes m}. \quad (60)$$

Combining i) and ii) we conclude that Eq. 50 holds true. \square

A.4 Proof of Lemma 4

Proof. The sub-matrices $A_{12}, A_{22}, A_{32}, A_{42}, A_{21}$ defined in Appendix B expressions (95) and (94) have all their elements different from ε . The sub-matrix A_{23} has all diagonal elements different from ε . As such, any node can be reached by any other node via the rows defined by $A_{12}, A_{22}, A_{32}, A_{42}$ and the columns defined by A_{21}, A_{22}, A_{23} . Therefore \bar{A} is irreducible. Since A is a similarity transformation away from \bar{A} then we conclude that A is also irreducible. \square

A.5 Proof of Lemma 5

Proof. We consider two cases:

i) $\tau_\gamma = \tau_\delta^{\otimes m} = \lambda$.

In this situation the circuits presented in Figs. 8a1 and 8a2 on page 20 all belong to the critical graph since their weights are τ_γ or $\tau_\delta^{\otimes m}$ both equal to the max-plus eigenvalue λ . Note that any circuit c_1 of length l made from the nodes of t_{ℓ_m} , illustrated in Fig. 8a1 on page 20, has an average weight of

$$\frac{|c_1|_w}{|c_1|_1} = \frac{(\tau_\delta^{\otimes m})^{\otimes l}}{l} = \tau_\delta^{\otimes m} = \lambda, \quad (61)$$

and as such also belongs to the critical graph.

Any other circuit in the precedence graph of \bar{A} must pass through at least one node of t_{ℓ_m} , as illustrated in Figs. 9b, c1, and c2 (with the exception of the self-loops in Fig. 8a3 and the circuits in Fig. 8a4 that we do not consider since their weights are e and $\tau_\gamma/2$ both less than λ). Additionally, arcs starting in nodes from a group t_{ℓ_q} with $q < m$ are only connected to nodes in ℓ_{ℓ_q+p} for $p \geq 0$ (or ℓ_{ℓ_q+p}). This is again illustrated in Figs. 9a, c1, and c2. Let $t_{[\ell_q]_i}$ denote element i of t_{ℓ_q} . Consider the circuit

$$c_2 : t_{[\ell_m]_i} \rightarrow t_{[\ell_q]_j} \rightarrow t_{[\ell_m]_i}, \quad (62)$$

with $q < m$. The average weight is (with $\tau_\gamma = \tau_\delta^{\otimes m}$)

$$\frac{|c_2|_w}{|c_2|_1} = \frac{\tau_\delta^{\otimes q} \otimes \tau_\gamma \otimes \tau_\delta^{\otimes (m-q)}}{2} = \frac{\tau_\delta^{\otimes m} \otimes \tau_\gamma}{2} = \lambda. \quad (63)$$

Circuit c_2 is thus also in the critical graph. For the general circuit of the type

$$c_3 : t_{[\ell_m]_i} \rightarrow \underbrace{t_{[\ell_{q_1}]_{j_1}} \rightarrow t_{[\ell_{q_2}]_{j_2}} \rightarrow \dots \rightarrow t_{[\ell_{q_l}]_{j_l}}}_{l \text{ nodes}} \rightarrow t_{[\ell_m]_i}, \quad (64)$$

with $q_1 < q_2 < \dots < q_l < m$, the average weight is

$$\begin{aligned} \frac{|c_3|_w}{|c_3|_1} &= \frac{\tau_\gamma^{\otimes l} \otimes \tau_\delta^{\otimes q_1} \otimes \tau_\delta^{\otimes (q_2 - q_1)} \otimes \dots \otimes \tau_\delta^{\otimes (m - q_l)}}{l + 1} \\ &= \frac{\tau_\gamma^{\otimes l} \otimes \tau_\delta^{\otimes m}}{l + 1} = \lambda. \end{aligned}$$

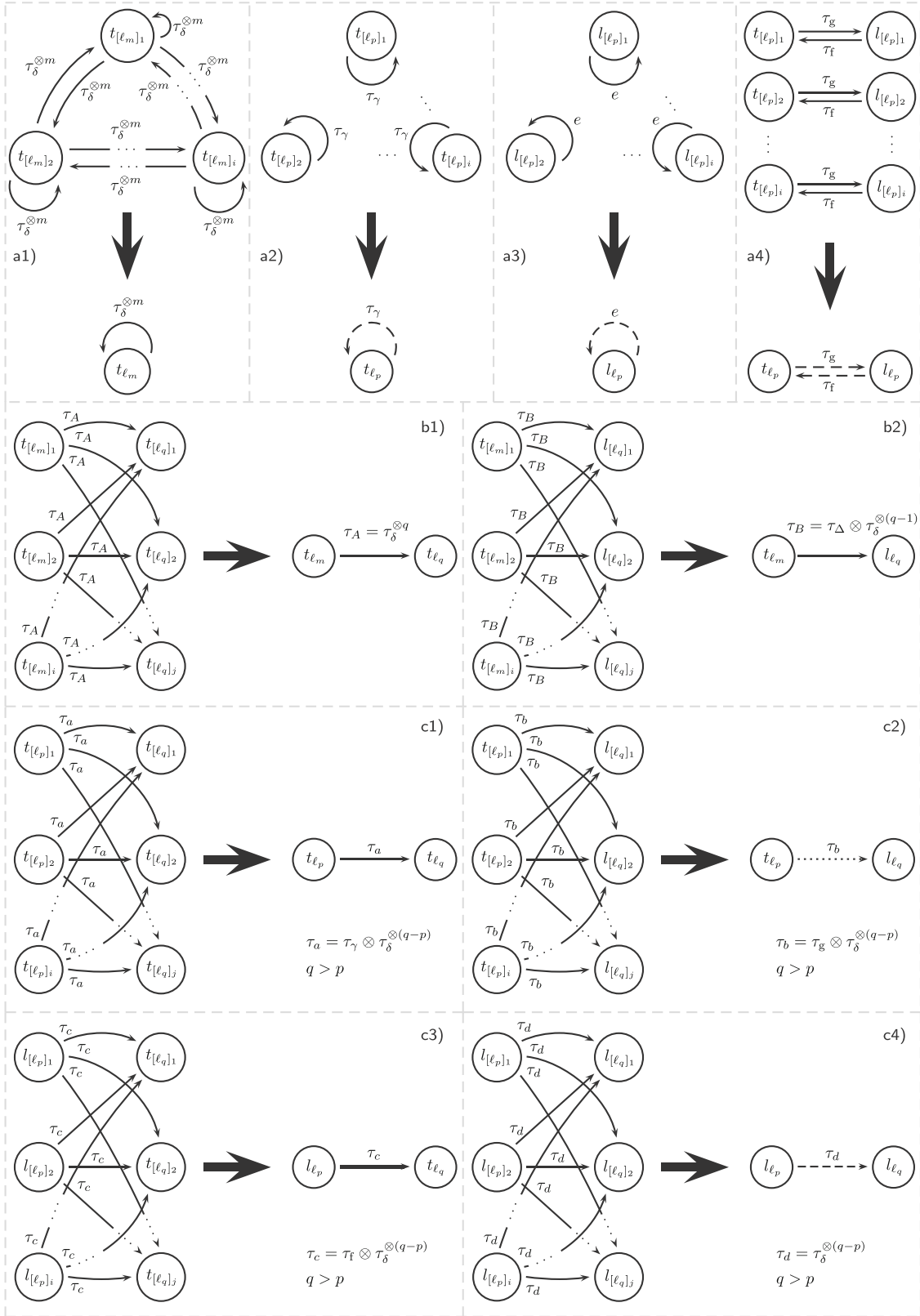


Figure 8: Graph reductions. Touchdown and lift off events with indexes belonging to the same set ℓ_q can be grouped together since they have the same number of output and input arcs with the same weights.

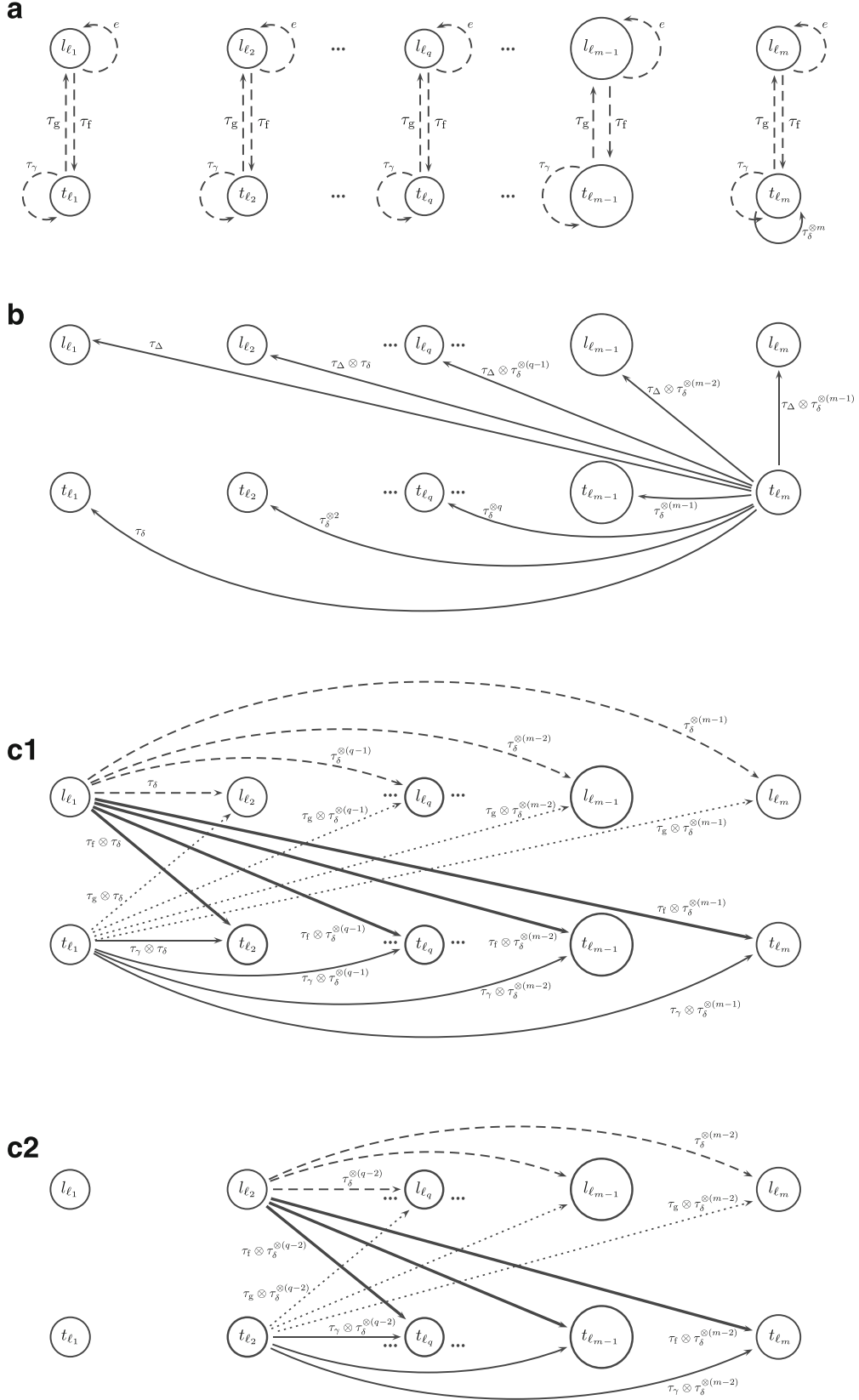


Figure 9: Elements of the precedence graph of the system matrix A . The total precedence graph of A is composed of all the arcs presented in a) and b), together with the $m - 1$ remaining subgraphs that follow the pattern of Figures c1) and c2).

Again, circuit c_3 is part of the critical graph. Any circuit that passes through any node in $l_{\ell q}$, for any q , will never be in the critical graph. This is due to the fact that arcs within touchdown nodes of different leg groups yield a higher weight:

$$t_{[\ell q]_i} \rightarrow t_{[\ell p]_j} \quad \text{weight: } \tau_\gamma \otimes \tau_\Delta^{\otimes(q-p)} \quad (65)$$

$$t_{[\ell q]_i} \rightarrow l_{[\ell p]_j} \quad \text{weight: } \tau_g \otimes \tau_\Delta^{\otimes(q-p)} \quad (66)$$

$$l_{[\ell q]_i} \rightarrow t_{[\ell p]_j} \quad \text{weight: } \tau_f \otimes \tau_\Delta^{\otimes(q-p)} \quad (67)$$

$$l_{[\ell q]_i} \rightarrow l_{[\ell p]_j} \quad \text{weight: } \tau_\Delta^{\otimes(q-p)}. \quad (68)$$

As such, a path that connects a touchdown node to a lift off node “loses” $\tau_\gamma - \tau_g = \tau_f$ from the maximum possible weight, a path from lift off to lift off nodes loses τ_γ , and a path from lift off nodes to touchdown nodes loses τ_g in weight. This can also be observed in the structure of \bar{A} , in Eq. 92, where the sub-matrix $\tau_f \otimes (\tau_g \otimes W \oplus V)$ overcomes the sub-matrices $\tau_g \otimes W \oplus V$, $\tau_f \otimes W$, and W . Consider, for example, the circuit c_4 :

$$c_4 : t_{[\ell m]_i} \rightarrow t_{[\ell p]_{j_0}} \rightarrow l_{[\ell p+q]_{j_q}} \rightarrow t_{[\ell m]_i} \quad (69)$$

then

$$\begin{aligned} \frac{|c_4|_w}{|c_4|_1} &= \frac{\tau_\delta^{\otimes p} \otimes (\tau_g \otimes \tau_\delta^{\otimes q}) \otimes (\tau_f \otimes \tau_\delta^{\otimes(m-(p+q))})}{3} \\ &= \frac{\tau_\gamma \otimes \tau_\delta^{\otimes m}}{3} < \lambda. \end{aligned}$$

Since all the nodes in the critical graph are connected (they are all touchdown nodes) we conclude that for the case $\tau_\gamma = \tau_\delta^{\otimes m} = \lambda$ the critical graph of \bar{A} has a single strongly connected subgraph. Figure 5a on page 14 illustrates the complete critical graph of \bar{A} for this case.

ii) $\tau_\gamma < \tau_\delta^{\otimes m} = \lambda$.

In this situation only circuits of the type c_1 are part of the critical graph. Circuits of the type c_2 or c_3 are not part of the critical graph. Figure 5b illustrates the resulting critical graph of \bar{A} . Since all the nodes of $t_{\ell m}$ are connected to each other we conclude that for the case $\tau_\gamma < \tau_\delta^{\otimes m} = \lambda$ the critical graph of \bar{A} has a single strongly connected subgraph.

A third case can be considered: $\tau_\delta^{\otimes m} < \tau_\gamma = \lambda$. In this situation the critical graph of \bar{A} does not have a single strongly connected subgraph. Figure 5c illustrates this situation, that we document here without proof. \square

A.6 Proof of Theorem 3

Proof. According to Lemma 4 the matrix A is irreducible, and as such it has a unique max-plus eigenvalue. According to Lemma 5 the critical graph of $\mathcal{G}^c(A)$ has a single strongly connected subgraph, and as such its max-plus eigenvector is unique up to a max-plus scaling factor (see Baccelli et al. (1992), Theorem 3.101). \square

A.7 Proof of Lemma 6

Proof. Computing successive products of \bar{A} and taking advantage of its structure, which can be found in Appendix B, and Eqs. 83–85 one can write its p -th power $\bar{A}^{\otimes p}$, valid for all $p \geq 2$, illustrated by Eqs. 72 and 74.

By inspection of the expression of $\bar{A}^{\otimes p}$ in Eqs. 72–74 one can observe that most terms are max-plus multiplying by a power of the max-plus eigenvalue λ (recall that with Assumption A2 we have $\lambda = \tau_\delta^{\otimes m}$). To factor out λ of the matrix composed by expressions Eqs. 72 and 74 we show that

$$\begin{aligned} \lambda^{\otimes(p-2)} \otimes \tau_f \otimes \tau_g \otimes V \otimes W &\geq \tau_f^{\otimes(p-1)} \otimes \tau_g^{\otimes p} \otimes W \Leftrightarrow \\ \tau_g \otimes \lambda^{\otimes(p-2)} \otimes \tau_f \otimes V \otimes W &\geq \tau_g \otimes \tau_\gamma^{\otimes(p-1)} \otimes W \end{aligned} \quad (70)$$

Since $\lambda \geq \tau_\gamma$ it is sufficient to show that

$$\tau_f \otimes V \otimes W \geq \tau_\gamma \otimes W \quad (71)$$

This can be confirmed by inspecting Eq. 88 and 76:

1. All the terms in the upper block triangle of $\tau_\gamma \otimes W$ are ε while for $\tau_f \otimes V \otimes W$ they are positive numbers.
2. In the block diagonal $[\tau_f \otimes V \otimes W]_{i,i} = \tau_\delta^{\otimes m} \otimes \mathbb{1} \geq \tau_\gamma \otimes E = [\tau_\gamma \otimes W]_{i,i}$, by Assumption A2.
3. In the lower block triangle $[\tau_f \otimes W \otimes W]_{i,j} = \tau_\delta^{\otimes(m+i-j)} \otimes \mathbb{1} \geq \tau_\delta^{\otimes(i-j)} \otimes \tau_\gamma \otimes \mathbb{1} = [\tau_\gamma \otimes W]_{i,j}$, by Assumption A2.

Taking advantage of this simplification one can obtain Eqs. 73, 75, and 77–79 (with \otimes omitted in unambiguous locations). Together with the similarity transformation we obtain the result valid for $p \geq 2$:

$$A^{\otimes(p+1)} = C \otimes \bar{A}^{\otimes(p+1)} \otimes C^T = C \otimes \lambda \otimes \bar{A}^{\otimes p} \otimes C^T = \lambda \otimes A^{\otimes p},$$

thus concluding that the coupling time is $k_0 z = 2$ with cyclicity $c = 1$.

$$[\bar{A}^{\otimes p}]_{\cdot,1} = \begin{bmatrix} \tau_f \left(\lambda^{\otimes(p-2)} \tau_f \tau_g V W \oplus \lambda^{\otimes(p-1)} V \oplus \tau_f^{\otimes(p-1)} \tau_g^{\otimes p} W \right) \\ \lambda^{\otimes(p-2)} \tau_f \tau_g V W \oplus \lambda^{\otimes(p-1)} V \oplus \tau_f^{\otimes(p-1)} \tau_g^{\otimes p} W \end{bmatrix} \quad (72)$$

$$= \begin{bmatrix} \tau_f \left(\lambda^{\otimes(p-2)} \tau_f \tau_g V W \oplus \lambda^{\otimes(p-1)} V \right) \\ \lambda^{\otimes(p-2)} \tau_f \tau_g V W \oplus \lambda^{\otimes(p-1)} V \end{bmatrix} \quad (73)$$

$$[\bar{A}^{\otimes p}]_{\cdot,2} = \begin{bmatrix} \tau_f \left(\ell^{\otimes(p-2)} \tau_f V W \oplus (\tau_f \tau_g)^{\otimes(p-1)} W \right) \\ \lambda^{\otimes(p-2)} \tau_f V W \oplus (\tau_f \tau_g)^{\otimes(p-1)} W \end{bmatrix} \quad (74)$$

$$= \begin{bmatrix} \tau_f \left(\lambda^{\otimes(p-2)} \tau_f V W \right) \\ \lambda^{\otimes(p-2)} \tau_f V W \end{bmatrix} \quad (75)$$

$$\tau_f \otimes V \otimes W = \begin{bmatrix} \tau_\delta^{\otimes m} \otimes \bar{\mathbb{1}}_{1,1} & \cdots & \tau_\delta \otimes \bar{\mathbb{1}}_{1,m} \\ \vdots & \ddots & \vdots \\ \tau_\delta^{\otimes(2m-1)} \otimes \bar{\mathbb{1}}_{m,1} & \cdots & \tau_\delta^{\otimes m} \otimes \bar{\mathbb{1}}_{m,m} \end{bmatrix} \quad (76)$$

$$\bar{A}^{\otimes(p+1)} = \begin{bmatrix} \tau_f \left(\lambda^{\otimes(p-1)} \tau_f \tau_g V W \oplus \lambda^{\otimes p} V \right) & \tau_f \left(\lambda^{\otimes(p-1)} \tau_f V W \right) \\ \lambda^{\otimes(p-1)} \tau_f \tau_g V W \oplus \lambda^{\otimes p} V & \lambda^{\otimes(p-1)} \tau_f V W \end{bmatrix} \quad (77)$$

$$= \lambda \otimes \begin{bmatrix} \tau_f \left(\lambda^{\otimes(p-2)} \tau_f \tau_g V W \oplus \lambda^{\otimes(p-1)} V \right) & \tau_f \left(\lambda^{\otimes(p-2)} \tau_f V W \right) \\ \lambda^{\otimes(p-2)} \tau_f \tau_g V W \oplus \lambda^{\otimes(p-1)} V & \lambda^{\otimes(p-2)} \tau_f V W \end{bmatrix} \quad (78)$$

$$= \lambda \otimes \bar{A}^{\otimes p} \quad (79)$$

□

B Structure of the system matrix \bar{A}

For an arbitrary gait the internal structure of A can be quite complex. However, the gait G associated to A can be transformed into a normal gait via a similarity transformation. Let

$$C = \begin{bmatrix} \bar{C} & \mathcal{E} \\ \mathcal{E} & \bar{C} \end{bmatrix}. \quad (80)$$

The similarity matrix C transforms the system matrix A of an arbitrary gait G into the system matrix \bar{A} of a normal gait \bar{G} via the similarity transformation

$$\bar{A} = C \otimes A \otimes C^T.$$

This can be shown by direct computation:

$$C \otimes A \otimes C^T = C \otimes A_0^* \otimes C^T \otimes C \otimes A_1 \otimes C^T = A_0^* \otimes \bar{A}_1 = \bar{A}.$$

Transforming an arbitrary gait into a normal gait is very useful since, by effectively switching rows and columns in A , one obtains a very structured matrix \bar{A} for which a structural analysis is much easier. The

interpretation of the similarity matrix \bar{C} is that legs can be renumbered, simplifying algebraic manipulation. Besides max-plus nilpotency, other properties are invariant to similarity transformations: irreducibility is preserved since the graphs of A and \bar{A} are equivalent up to a label renaming. Max-plus eigenvalues and eigenvectors are related by:

$$\begin{aligned} A \otimes \nu &= \lambda \otimes \nu \\ \Leftrightarrow C \otimes A \otimes C^T \otimes C \otimes \nu &= \lambda \otimes C \otimes \nu \\ \Leftrightarrow \bar{A} \otimes \bar{\nu} &= \lambda \otimes \bar{\nu}, \text{ with } \bar{\nu} = C \otimes \nu. \end{aligned}$$

The structure of \bar{A} can be obtained via a laborious but straightforward set of algebraic manipulations. For an arbitrary gait G we compute the normal gait \bar{G} via the similarity transformation with the matrix C . By observing the structures of \bar{A}_0^* and \bar{A}_1 (derived from \bar{P} and \bar{Q}) a closed-form solution can be obtained for \bar{A}_0^* :

$$\bar{A}_0^* = \begin{bmatrix} W & \tau_f \otimes W \\ \bar{W} & W \end{bmatrix}, \quad (81)$$

where $W = (\tau_f \otimes P)^*$, illustrated in Eq. 88 on page 25. The matrix \bar{W} is defined in Eq. 87 on page 12. Note that $\tau_f \otimes \bar{W} \oplus E = W$ and $W \geq \bar{W}$. An expression for \bar{A} is then obtained:

$$\begin{aligned} \bar{A} &= \bar{A}_0^* \otimes \bar{A}_1 = \begin{bmatrix} W & \tau_f \otimes W \\ \bar{W} & W \end{bmatrix} \otimes \begin{bmatrix} E & \mathcal{E} \\ \tau_g \otimes E \oplus \bar{Q} & E \end{bmatrix} \\ &= \begin{bmatrix} W \oplus \tau_f \otimes \tau_g \otimes W \oplus \tau_f \otimes W \otimes \bar{Q} & \tau_f \otimes W \\ \bar{W} \oplus \tau_g \otimes W \oplus W \otimes \bar{Q} & W \end{bmatrix}. \end{aligned} \quad (82)$$

Let $V = W \otimes \bar{Q}$, as illustrated by Eq. 89. One can show that:

$$W \otimes W = W \quad (83)$$

$$W \otimes V = V \quad (84)$$

$$V \otimes V = \tau_\delta^{\otimes(m-1)} \otimes \tau_\Delta \otimes V \quad (85)$$

Since $\mu \otimes V \geq W$ for any $\mu > 0$, and $W \geq \bar{W}$, expression (82) simplifies to:

$$\bar{A} = \begin{bmatrix} \tau_f \otimes (\tau_g \otimes W \oplus V) & \tau_f \otimes W \\ \tau_g \otimes W \oplus V & W \end{bmatrix}. \quad (86)$$

Let

$$\begin{aligned} t_{\ell_i}(k) &= [t_{[\ell_i]_1}(k) t_{[\ell_i]_2}(k) \cdots t_{[\ell_i]_{\#\ell_i}}(k)]^T \\ l_{\ell_i}(k) &= [l_{[\ell_i]_1}(k) l_{[\ell_i]_2}(k) \cdots l_{[\ell_i]_{\ell_i}}(k)]^T. \end{aligned}$$

Equations 90–93 illustrate the resulting structure of \bar{A} written in the system form $\bar{x}(k) = \bar{A} \otimes \bar{x}(k-1)$, with $\bar{x}(k) = C \otimes x(k)$, and $\bar{E}_i = E_{\#\ell_i}$.

$$W = \tau_{\Delta} \otimes \begin{bmatrix} \mathcal{E} & & \cdots & \mathcal{E} \\ \bar{\mathbb{I}}_{2,1} & \mathcal{E} & & \vdots \\ \tau_{\delta} \otimes \bar{\mathbb{I}}_{3,1} & \bar{\mathbb{I}}_{3,2} & \mathcal{E} & \\ \vdots & \ddots & \ddots & \\ \tau_{\delta}^{\otimes(m-2)} \otimes \bar{\mathbb{I}}_{m,1} & \cdots & \tau_{\delta} \otimes \bar{\mathbb{I}}_{m,m-1} & \bar{\mathbb{I}}_{m,m-2} & \mathcal{E} \end{bmatrix} \quad (87)$$

$$W = \begin{bmatrix} \bar{E}_1 & & \cdots & \mathcal{E} \\ \tau_{\delta} \otimes \bar{\mathbb{I}}_{2,1} & \bar{E}_2 & & \vdots \\ \tau_{\delta}^{\otimes 2} \otimes \bar{\mathbb{I}}_{3,1} & \tau_{\delta} \otimes \bar{\mathbb{I}}_{3,2} & \bar{E}_3 & \\ \vdots & \ddots & \ddots & \\ \tau_{\delta}^{\otimes(m-1)} \otimes \bar{\mathbb{I}}_{m,1} & \cdots & \tau_{\delta}^{\otimes 2} \otimes \bar{\mathbb{I}}_{m,m-2} & \tau_{\delta} \otimes \bar{\mathbb{I}}_{m,m-1} & \bar{E}_m \end{bmatrix} \quad (88)$$

$$V = \left[\begin{array}{c|ccc} \mathcal{E}_{n,(n-m)} & \tau_{\Delta} \otimes \bar{\mathbb{I}}_{1,m} & & \\ & \tau_{\Delta} \otimes \tau_{\delta} \otimes \bar{\mathbb{I}}_{2,m} & & \\ & \vdots & & \\ & \tau_{\Delta} \otimes \tau_{\delta}^{\otimes(m-1)} \otimes \bar{\mathbb{I}}_{m,m} & & \end{array} \right] \quad (89)$$

With (the \otimes operator is omitted in unambiguous locations):

$$\bar{x}(k) = \bar{A} \otimes \bar{x}(k-1) \Leftrightarrow \quad (90)$$

$$\bar{x}(k) = \left[\begin{array}{c|c} \tau_{\mathbb{f}} \otimes (\tau_{\mathbb{g}} \otimes W \oplus V) & \tau_{\mathbb{f}} \otimes W \\ \hline \tau_{\mathbb{g}} \otimes W \oplus V & W \end{array} \right] \otimes \bar{x}(k-1) \Leftrightarrow \quad (91)$$

$$\underbrace{\begin{bmatrix} t_{\ell_1}(k) \\ \vdots \\ t_{\ell_m}(k) \\ \hline l_{\ell_1}(k) \\ \vdots \\ l_{\ell_m}(k) \end{bmatrix}}_{\bar{x}(k)} = \underbrace{\begin{bmatrix} A_{11} & A_{12} & A_{13} \\ \hline A_{21} & A_{22} & A_{23} \\ \hline A_{31} & A_{32} & A_{33} \\ \hline A_{41} & A_{42} & A_{43} \end{bmatrix}}_{\bar{A}} \otimes \underbrace{\begin{bmatrix} t_{\ell_1}(k-1) \\ \vdots \\ t_{\ell_m}(k-1) \\ \hline l_{\ell_1}(k-1) \\ \vdots \\ l_{\ell_m}(k-1) \end{bmatrix}}_{\bar{x}(k-1)} \quad (92)$$

$$\left[\begin{array}{c|c} A_{11} & A_{12} \\ \hline A_{21} & A_{22} \end{array} \right] = \left[\begin{array}{ccc|c} \tau_{\gamma} \bar{E}_1 & \cdots & \mathcal{E} & \tau_{\delta} \bar{\mathbb{I}}_{1,m} \\ \tau_{\gamma} \tau_{\delta} \bar{\mathbb{I}}_{2,1} & \tau_{\gamma} \bar{E}_2 & \vdots & \tau_{\delta}^{\otimes 2} \bar{\mathbb{I}}_{2,m} \\ \vdots & \ddots & \ddots & \vdots \\ \hline \tau_{\gamma} \tau_{\delta}^{\otimes(m-1)} \bar{\mathbb{I}}_{m,1} & \cdots & \tau_{\gamma} \tau_{\delta} \bar{\mathbb{I}}_{m,m-1} & \tau_{\gamma} \bar{E}_m \oplus \tau_{\delta}^{\otimes m} \bar{\mathbb{I}}_{m,m} \end{array} \right] \quad (93)$$

$$\left[\begin{array}{c|c} A_{31} & A_{32} \\ \hline A_{41} & A_{42} \end{array} \right] = \left[\begin{array}{ccc|c} \tau_{\mathbb{g}} \bar{E}_1 & \cdots & \mathcal{E} & \tau_{\Delta} \bar{\mathbb{I}}_{1,m} \\ \tau_{\mathbb{g}} \tau_{\delta} \bar{\mathbb{I}}_{2,1} & \tau_{\mathbb{g}} \bar{E}_2 & \vdots & \tau_{\Delta} \tau_{\delta} \bar{\mathbb{I}}_{2,m} \\ \vdots & \ddots & \ddots & \vdots \\ \hline \tau_{\mathbb{g}} \tau_{\delta}^{\otimes(m-1)} \bar{\mathbb{I}}_{m,1} & \cdots & \tau_{\mathbb{g}} \tau_{\delta} \bar{\mathbb{I}}_{m,m-1} & \tau_{\mathbb{g}} \bar{E}_m \oplus \tau_{\Delta} \tau_{\delta}^{\otimes(m-1)} \bar{\mathbb{I}}_{m,m} \end{array} \right] \quad (94)$$

$$\begin{bmatrix} A_{13} \\ A_{23} \\ A_{33} \\ A_{43} \end{bmatrix} = \begin{bmatrix} \tau_f \bar{E}_1 & \cdots & \mathcal{E} \\ \tau_f \tau_\delta \bar{\mathbb{1}}_{2,1} & \tau_f \bar{E}_2 & \vdots \\ \vdots & \ddots & \\ \tau_f \tau_\delta^{\otimes(m-1)} \bar{\mathbb{1}}_{m,1} & \cdots & \tau_f \bar{E}_m \\ \hline \bar{E}_1 & \cdots & \mathcal{E} \\ \tau_\delta \bar{\mathbb{1}}_{2,1} & \bar{E}_2 & \vdots \\ \vdots & \ddots & \\ \tau_\delta^{\otimes(m-1)} \bar{\mathbb{1}}_{m,1} & \cdots & \bar{E}_m \end{bmatrix} \quad (95)$$

C Precedence Graph of \bar{A}

With the structure given it is possible to construct the precedence graph of \bar{A} . Since this graph can be quite large for a general \bar{A} , we find it more efficient to first group “similar” nodes into a single node, i.e. apply a procedure called node reduction (Fig. 8 on page 20).

Next, we show various subgraphs of the graph of \bar{A} to better illustrate its structure (Fig. 9 on page 21). The total precedence graph of \bar{A} is thus the combination of Figs. 8 and 9.

The process of constructing the graph of \bar{A} starts by grouping all nodes of an event associated with a group of legs ℓ_i into a single node. This can be accomplished since event nodes from the same group of legs ℓ_i have “similar” incoming and outgoing arcs. As an example, consider the first set of $\#\ell_1$ rows of \bar{A} as defined in expression (89):

$$\begin{aligned} t_{\ell_1}(k) = & \tau_\gamma \otimes E_1 \otimes t_{\ell_1}(k-1) \oplus \tau_\delta \otimes \mathbb{1}_{1,m} \otimes t_{\ell_m}(k-1) \oplus \\ & \tau_\delta \otimes E_1 \otimes l_{\ell_1}(k-1). \end{aligned} \quad (96)$$

The precedence graph for Eq. 96 consists of $3 \times \#\ell_1$ nodes, since it involves the vectors t_{ℓ_1} , t_{ℓ_m} , and l_{ℓ_1} . The relation between $t_{\ell_1}(k)$ and $t_{\ell_1}(k-1)$ results in $\#\ell_1$ self connected arcs in the t_{ℓ_1} events with weights τ_γ . Instead of expressing all elements of t_{ℓ_1} as individual nodes with self arcs, we reduce then to a single node with one self arc, as seen in Fig. 8a2. The dashed attribute used on the self arc indicates that for each node in the group only self arcs exist, as expressed by the “connecting” matrix E_1 . The relation between $t_{\ell_1}(k)$ and $t_{\ell_m}(k-1)$ is somewhat more involved, since it contains $\#\ell_1 \times \#\ell_m$ arcs, as expressed by the connecting matrix $\mathbb{1}_{1,m}$. The resulting node reduction is illustrated in Fig. 8b1. The node reduction for the relation between t_{ℓ_1} and l_{ℓ_1} is illustrated in Fig. 8a4. Again we use dashed attributes on the arcs to represent the connecting matrix E_1 . For all other relations with connecting matrices $\mathbb{1}$ we use solid arcs. We make an exception in Figs. 8c1 to c4 where different line attributes are used to distinguish arcs from $t_{\ell_p} \rightarrow t_{\ell_q}$, $t_{\ell_p} \rightarrow l_{\ell_q}$, etc. The same line attributes are used in Figs. 9c1 and c2. Note that multiple incoming arcs to a node are related via the \oplus operation, e.g. as in the example Eq. 96 the node t_{ℓ_1} has 3 incoming arcs, illustrated in Fig. 9.

The following list summarizes the node reduction:

- Figure 8a1 illustrates node reduction of the term $\tau_\delta^{\otimes m} \otimes \mathbb{1}_{m,m}$ of sub-matrix A_{22} from expression (95).
- Figure 8a2 illustrates the node reduction of the block diagonal of matrix A_{11} and the $\tau_\gamma \otimes \bar{E}_m$ term of A_{22} .
- Figure 8a3 illustrates the node reduction of the block diagonal of matrix $[A_{33}^T \ A_{43}^T]^T$.
- Figure 8a4 illustrates the node reduction of the term $\tau_g \otimes E_m$ of sub-matrix A_{42} together with the block diagonals of matrices A_{31} and $[A_{13}^T \ A_{23}^T]^T$.
- Figures 8b1 and b2 illustrate the node reduction for the columns formed by the matrices (not including the term $\tau_g \otimes E_m$ from matrix A_{42} already represented in Fig. 8a4) A_{12} and $[A_{32}^T \ A_{42}^T]^T$ respectively.
- Figures 8c1 to c4 illustrate the node reduction of the off-diagonal elements of matrices $\tau_\gamma \otimes W$, $\tau_f \otimes W$, $\tau_g \otimes W$, and W , from expression (92) respectively. Given the node reduction one can now proceed to construct the precedence graph of \bar{A} :

- Figure 9a is the graph of the block diagonal of \bar{A} together with the block diagonals of the sub-matrices $\begin{bmatrix} A_{31} & A_{32} \\ A_{41} & A_{42} \end{bmatrix}$ and $\begin{bmatrix} A_{13}^T & A_{23}^T \end{bmatrix}^T$ using the node reductions presented in Figs. 8a1 to a4.
- Figure 9b is the graph of the columns formed by the matrices A_{12} and $\begin{bmatrix} A_{32}^T & A_{42}^T \end{bmatrix}^T$ using node reductions presented in Figs. 8b1 and b2.
- Figures 9c1 and c2 illustrate two subgraphs of the remaining columns of \bar{A} . Note that we only present the subgraphs of the first sets of $\#\ell_1$ and $\#\ell_2$ out of a total of $m - 1$ columns. These follow the same pattern. We use different attributes on the arcs, such as dashed, thick solid, etc., to distinguish the different node reductions, as presented in Figs. 8c1 to c4.

References

- Baccelli F, Cohen G, Olsder G, Quadrat J (1992) Synchronization and Linearity: an Algebra for Discrete Event Systems. Wiley
- Bede B, Nobuhara H (2009) A novel max-plus algebra based wavelet transform and its applications in image processing. In: Proceedings of the IEEE International Conference on Systems, Man and Cybernetics. San Antonio, Texas, pp 2585–2588
- Braker J (1991) Max-algebra modelling and analysis of time-table dependent transportation networks. In: Proceedings of the First European Control Conference, Grenoble, France
- Braker J, Olsder G (1993) The power algorithm in max algebra. *Linear Algebra Appl* 182:67–89
- Cohen A, Rossignol S, Grillner S (1988) Neural control of rhythmic movements in vertebrates. Wiley
- Cohen G, Dubois D, Quadrat J, Viot M (1983) A linear-system-theoretic view of discrete-event processes. In: Proceedings of the 22nd IEEE Conference on Decision and Control. San Antonio, Texas, pp 1039–1044
- Cohen G, Dubois D, Quadrat J, Viot M (1985) A linear-system-theoretic view of discrete-event processes and its use for performance evaluation in manufacturing. *IEEE Trans Autom Control* 30(3):210–220
- Cohen G, Moller P, Quadrat J, Viot M (1989) Algebraic tools for the performance evaluation of discrete event systems. *Proc IEEE* 77(1):39–58
- Cuninghame-Green R (1961) Process synchronisation in a steelworks – A problem of feasibility. In: Banbury J, Maitland J (eds) Proceedings of the 2nd international conference on operational research. London: English Universities Press, Aix-en-Provence, pp 323–328
- Cuninghame-Green R (1962) Describing industrial processes with interference and approximating their steady-state behaviour. *Oper Res Q* 13(1):95–100
- Cuninghame-Green R (1979) Minimax algebra, lecture notes in economics and mathematical systems, vol 166. Springer-Verlag
- De Schutter B, van den Boom T (2008) Max-plus algebra and max-plus linear discrete event systems: An introduction. In: Proceedings of the 9th International Workshop on Discrete Event Systems, Göteborg, Sweden, pp 36–42
- Dorfler F, Bullo F (2012) Exploring synchronization in complex oscillator networks. In: IEEE Conference on Decision and Control, pp 7157–7170
- Full R, Koditschek D (1999) Templates and anchors: neuromechanical hypotheses of legged locomotion on land. *J Exp Biol* 202(23):3325–3332
- Gaubert S (1990) An algebraic method for optimizing resources in timed event graphs. In: Bensoussan A, Lions J (eds) Proceedings of the 9th International Conference on Analysis and Optimization of Systems, Berlin, Germany: Springer-Verlag, Antibes, France, Lecture Notes in Control and Information Sciences, vol 144, pp 957–966
- Gaubert S (1992) Théorie des systèmes linéaires dans les dioides. PhD thesis, Ecole Nationale Supérieure des Mines de Paris, France
- Gaubert S (1993) Timed automata and discrete event systems. In: Proceedings of the 2nd European Control Conference, Groningen, The Netherlands
- Gaubert S (1994) On rational series in one variable over certain dioids. Technical Report 2162, INRIA, Le Chesnay, France
- Gaubert S, Mairesse J (1998) Task resource models and $(\max, +)$ automata. In: Gunawardena J (ed) Idempotency. Cambridge University Press
- Gaubert S, Plus M (1997) Methods and applications of $(\max, +)$ linear algebra. In: Proceedings of the symposium on theoretical aspects of computer science. Aachen, Germany, pp 261–282

- Giffler B (1960) Mathematical solution of production planning and scheduling problems. Technical Report IBM ASDD
- Giffler B (1963) Scheduling general production systems using schedule algebra. *Nav Res Logisti Q* 10(3):237–255
- Giffler B (1968) Schedule algebra: a progress report. *Nav Res Logist Q* 15(2):255–280
- Gondran M, Minoux M (1976) Eigenvalues and eigenvectors in semimodules and their interpretation in graph theory. In: *Proceedings of the 9th International Mathematical Programming Symposium, Budapest, Hungary*, pp 333–348
- 258 *Discrete Event Dyn Syst* (2016) 26:225–261
- Gondran M, Minoux M (1984) Linear algebra in dioids: a survey of recent results. *Ann Discrete Math* 19:147–163
- Gondran M, Minoux M (1987) Dioïd theory and its applications. In: *Algèbres Exotiques et Systèmes à Événements Discrets, CNRS/CNET/INRIA Seminar, CNET, Issy-les-Moulineaux, France*, pp 57–75
- Grillner S (1985) Neurobiological bases of rythmic motor acts in vertebrates. *Science* 228(4696):143–149
- Grillner S (2011) Control of locomotion in bipeds, tetrapods, and fish. *Comprehensive Physiology Supplement 2: Handbook of Physiology, The Nervous System, Motor Control*, pp 1179–1236
- Haynes G, Cohen F, Koditschek D (2009) Gait transitions for quasi-static hexapedal locomotion on level ground. In: *Proceedings of the International Symposium of Robotics Research, Lucerne, Switzerland*, pp 105–121
- Heidergott B (2000) A characterisation of $(\max,+)$ -linear queueing systems. *Queueing Syst Theory Appl* 35:237–262
- Heidergott B, de Vries R (2001) Towards a $(\max,+)$ control theory for public transportation networks. *Discret Event Dyn Syst* 11:371–398
- Heidergott B, Olsder G, van der Woude J (2006) *Max plus at work: Modeling and analysis of synchronized systems*. Kluwer
- Hildebrand M (1965) Symmetrical gaits of horses. *Science* 150(3697):701–708
- Holmes P, Full R, Koditschek D, Guckenheimer J (2006) The dynamics of legged locomotion: models, analyses, and challenges. *SIAM Rev* 48(2):207–304
- Ijspeert A (2008) Central pattern generators for locomotion control in animals and robots: A review. *Neural Netw* 21(4):642–653
- Karp R (1978) A characterization of the minimum cycle mean in a digraph. *Discret Math* 23(3):309–311
- Klavins E, Koditschek D (2002) Phase regulation of decentralized cyclic robotic systems. *Int J Robot Res* 21(3):257–275
- Lopes G, Babuška R, De Schutter B, van den Boom T (2009) Switching max-plus models for legged locomotion. In: *Proceedings of the IEEE International Conference on Robotics and Biomimetics, Guilin, China*, pp 221–226
- Lopes G, Kersbergen B, van den Boom T, De Schutter B, Babuska R (2014) Modeling and control of legged locomotion via switching max-plus models. *IEEE Trans Robot* 30(3):652–665
- Muybridge E (1901) *The Human Figure in Motion*. Dover Publications
- Olsder G (1986) On the characteristic equation and minimal realizations for discrete-event dynamic systems. In: *Proceedings of the 7th International Conference on Analysis and Optimization of Systems, Antibes, France, Lecture Notes in Control and Information Sciences, vol 83*, pp 189–201
- Olsder G, Roos C (1988) Cramer and Cayley-Hamilton in the max algebra. *Linear Algebra Appl* 101:87–108
- Olsder G, Resing J, de Vries R, Keane M, Hooghiemstra G (1990) Discrete event systems with stochastic processing times. *IEEE Trans Autom Control* 35(3):299–302
- Peterson J (1981) *Petri Net Theory and the Modeling of Systems*. Englewood Cliffs, New Jersey: Prentice Hall, Inc.
- Raibert M (1986) *Legged robots that balance*. MIT Press, Cambridge
- Raibert M, Jr HB, Chepponis M, Koechling J, Hodgins J, Dustman D, Brennan W, Barrett D, Thompson C, Hebert J, Lee W, Borvansky L (1989) Dynamically stable legged locomotion. Technical Report 1179, MIT
- Saranli U, Buehler M, Koditschek D (2001) RHex: a simple and highly mobile hexapod robot. *Int J Robot Res* 20(7):616–631
- Shedden K (2002) Analysis of cell-cycle gene expression in *Saccharomyces cerevisiae* using microarrays and multiple synchronization methods. *Nucleic Acids Res* 30(13):2920–2929
- Weingarten J, Groff R, Koditschek D (2004) A framework for the coordination of legged robot gaits. In: *Proceedings of the IEEE Conference on Robotics, Automation and Mechatronics, Singapore*, pp 679–686
- Yamaguchi S (2003) Synchronization of cellular clocks in the suprachiasmatic nucleus. *Science* 302(5649):1408–1412
- Zhou M, DiCesare F, Desrochers A (1992) A hybrid methodology for synthesis of Petri net models for manufacturing systems. *IEEE Trans Robot Autom* 8(3):350–361